Karyappa *et al. Energy Mater.* **2025**, *5*, 500037
DOI: 10.20517/energymater.2024.149

Energy Materials

Review

Open Access

Check for updates

Unlocking the potential of liquid crystals as phase change materials for thermal energy storage

Rahul Karyappa[1,#], Johnathan Lee Joo Cheng[1,#], Charissa Lixuan Ho[2], Suxi Wang[1], Warinton Thitsartarn[1], Junhua Kong[1], Dan Kai[1], Beng Hoon Tan[1], Pei Wang[1], Zhengyao Qu[3], Xian Jun Loh[1], Jianwei Xu[1,4,5,*], Qiang Zhu[1,2,*]

[1]Institute of Materials Research and Engineering (IMRE), Agency for Science, Technology and Research (A*STAR), Singapore 138634, Singapore.
[2]School of Chemistry, Chemical Engineering and Biotechnology, Nanyang Technological University, Singapore 637371, Singapore.
[3]State Key Laboratory of Silicate Materials for Architectures, Wuhan University of Technology, Wuhan 430070, Hubei, China.
[4]Institute of Sustainability for Chemicals, Energy and Environment (ISCE[2]), Agency for Science, Technology and Research (A*STAR), Singapore 627833, Singapore.
[5]Department of Chemistry, National University of Singapore, Singapore 117543, Singapore.
[#]Authors contributed equally.

***Correspondence to:** Dr. Jianwei Xu, Institute of Sustainability for Chemicals, Energy and Environment (ISCE2), Agency for Science, Technology and Research (A*STAR), 1 Pesek Road, Jurong Island, Singapore 627833, Singapore. E-mail: xu_jianwei@isce2.a-star.edu.sg; Dr. Qiang Zhu, Institute of Materials Research and Engineering (IMRE), Agency for Science, Technology and Research (A*STAR), 2 Fusionopolis Way, Innovis #08-03, Singapore 138634, Singapore. E-mail: zhuq@imre.a-star.edu.sg

How to cite this article: Karyappa, R.; Lee Joo Cheng, J.; Lixuan Ho, C.; Wang, S.; Thitsartarn, W.; Kong, J.; Kai, D.; Tan, B. H.; Wang, P.; Qu, Z.; Loh, X. J.; Xu, J.; Zhu, Q. Unlocking the potential of liquid crystals as phase change materials for thermal energy storage. *Energy Mater.* **2025**, *5*, 500037. https://dx.doi.org/10.20517/energymater.2024.149

Received: 31 Aug 2024 **First Decision:** 21 Nov 2024 **Revised:** 12 Dec 2024 **Accepted:** 27 Dec 2024 **Published:** 23 Jan 2025

Academic Editor: Yuping Wu **Copy Editor:** Fangling Lan **Production Editor:** Fangling Lan

Abstract

This review paper examines the innovative use of liquid crystals (LCs) as phase change materials in thermal energy storage systems. With the rising demand for efficient energy storage, LCs offer unique opportunities owing to their tunable phase transitions, high latent heat, and favorable thermal conductivity. This paper covers various types of LCs, such as nematic, smectic, and cholesteric phases, and their roles in enhancing thermal energy storage. It discusses the mechanisms of LC phase transitions and their impact on energy storage efficiency. Strategies to improve the thermal conductivities of LCs and LC polymers have also been explored. One method involves embedding LC units within the molecular structure to promote orderly arrangement, facilitate heat flow, and reduce phonon scattering. Aligning polymer chains through external fields or mechanical processes significantly improves intrinsic thermal conductivity. The inclusion of thermally conductive fillers and optimization of filler-

© The Author(s) 2025. **Open Access** This article is licensed under a Creative Commons Attribution 4.0 International License (https://creativecommons.org/licenses/by/4.0/), which permits unrestricted use, sharing, adaptation, distribution and reproduction in any medium or format, for any purpose, even commercially, as long as you give appropriate credit to the original author(s) and the source, provide a link to the Creative Commons license, and indicate if changes were made.

matrix interactions further boost thermal performance. Challenges related to the scalability, cost-effectiveness, and long-term stability of LC-based phase change materials are addressed, along with future research directions. This review synthesizes the current knowledge and identifies gaps in the literature, providing a valuable resource for researchers and engineers to develop advanced thermal energy storage technologies, contributing to sustainable energy solutions.

Keywords: Liquid crystals, liquid crystal polymers, phase change material, thermal conductivity, thermal energy storage

INTRODUCTION

The urgent need to reduce reliance on fossil fuels and mitigate the environmental harm caused by carbon emissions has increased the demand for renewable and sustainable energy sources[1-4]. Thermal energy storage (TES) systems serve as promising alternatives by enabling the storage of excess heat as latent heat energy, which can be utilized in the future[5-8]. A solar energy power plant is a common example of TES[9,10]. Such plants can be designed and operated economically and efficiently, if the surplus energy stored during the daytime is kept for utilization later. To this end, phase change materials (PCMs) are of great importance in improving thermal control of buildings[11,12] owing to their desirable properties that allow for the storage and release of a significant amount of latent heat when it changes from one physical state to another at a nearly constant temperature [Figure 1A-i]. By undergoing a phase change, these materials can exchange latent heat with their surroundings, thereby reducing temperature fluctuations[13-15]. PCMs primarily store excess heat that accumulates at higher temperatures and then release stored heat at lower temperatures [Figure 1A-ii]. Thus, the temperature of the PCMs strongly corresponds to the efficiency of the storage system[2].

A PCM absorbs significant amount of energy during its phase transition, typically from a solid to liquid state (endothermic process). It is then released during the transformation back to the solid form (exothermic process) when the ambient temperature falls below its melting point [Figure 1A-ii][16-19]. Typically, PCMs behave in a manner similar to other materials which store sensible heat beyond the phase-change region (solid + liquid region in Figure 1A-i). In the phase-change process, the heat of storage (DQ) can be estimated from the difference in enthalpy (DH) of the solid and the liquid phases (DQ = DH). Solid-liquid PCMs are the most efficient among different types of PCMs (e.g., solid-solid and solid-gas), as they absorb the most heat during the phase transitions for the smallest change in volume (< 10%)[18,20,21]. It is necessary to encapsulate these PCMs inside the protective shell material to avoid their interaction with the surroundings when in liquid state[22]. They can be organic (e.g., paraffins and fatty acids) or inorganic (e.g., salt hydrates and metallic alloys) materials.

As an alternative to these solid-liquid PCMs, liquid crystals (LC) have emerged as a promising alternative as they offer unique thermophysical properties and tunable phase transition temperatures (T_p) particularly suitable for use in TES[23,24]. LCs are substances that exhibit a unique state of matter that combines the properties of both liquids and solid crystals[25]. LCs consist of rod-like or disc-shaped molecules that exhibit a degree of orientational order while still flowing as a liquid[26,27]. There are two main types of LCs: lyotropic and thermotropic [Figure 1B]. Lyotropic LCs are formed when amphiphilic molecules dissolve in a suitable solvent, such as water. Their properties are predominantly dependent on the concentration of these molecules and additional factors, including temperature and pH[28]. Lyotropic LCs can exhibit various phases beyond the critical micelle concentration (CMC), resulting in structures such as micelles, hexagonal phases, lamellar phases, and bicontinuous cubic phases, each characterized by distinct arrangements of amphiphilic molecules arising from the equilibrium between hydrophilic and hydrophobic interactions. For

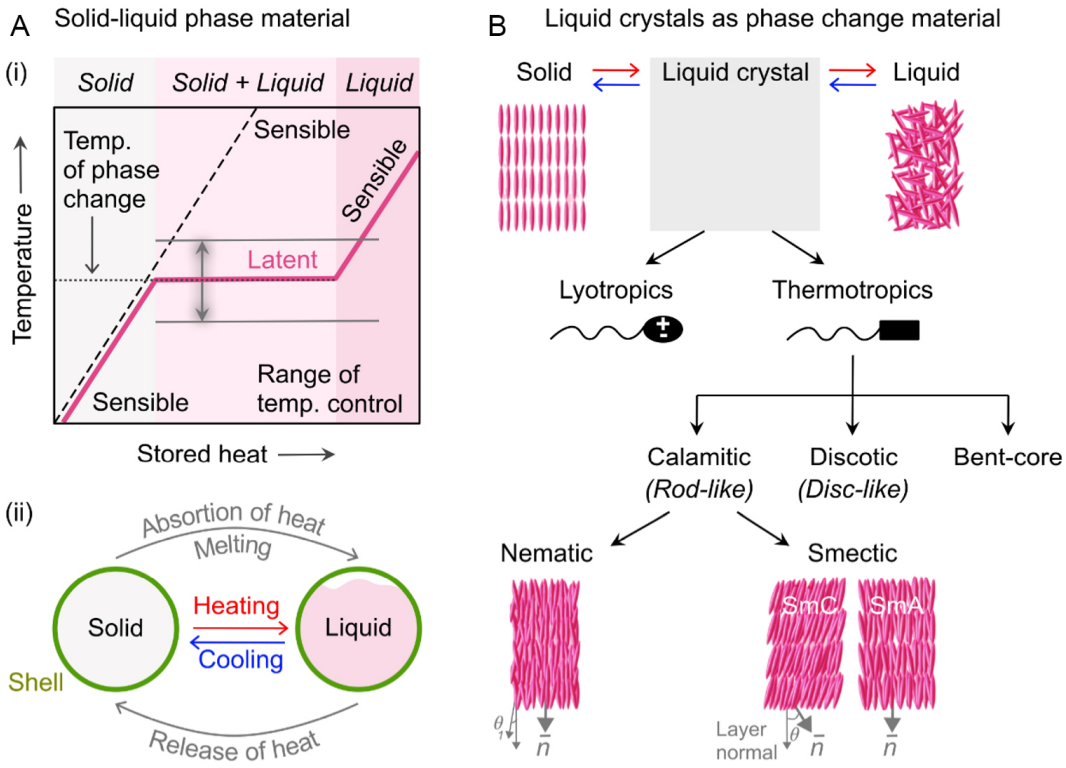

Figure 1. (A-i) Graphical representation of principles of phase change of phase change materials (PCM), and (A-ii) schematic representation of phase change process in solid-liquid PCMs. (B) Classification of liquid crystals (LC). Typical phases of thermotropic LCs with the increase in temperature from crystal phase to liquid (isotropic, I) phase.

instance, the lamellar phase consists of alternating lipid bilayers and water, whereas the bicontinuous cubic phase exhibits a three-dimensional (3D) honeycomb structure.

In contrast to lyotropic LCs, thermotropic LCs change their phase in response to temperature variations, with three primary mesophases: nematic, smectic, and cholesteric. Nematic LCs have molecules that align in a common direction but lack positional order. Smectic LCs form layered structures, with molecules aligned within each layer. Cholesteric LCs, also known as chiral nematic LCs, have a helical arrangement of molecules that gives them unique optical properties. The distinct properties of each type of LC make them suitable for various applications, including display technologies[29-32] and sensors[33-35].

Among the different types of LCs, thermotropic LCs possess characteristics that make them suitable for TES applications[23,36]. These crystals exhibit reversible phase transitions at specific temperatures, enabling them to absorb or release latent heat. Moreover, they remain in a liquid state throughout the phase change process, thereby mitigating issues such as supercooling and phase separation, which are commonly associated with conventional solid-liquid PCMs [Table 1]. The transition of LCs from one mesophase to another, such as from the nematic to the smectic or cholesteric phases [Figure 1B], can be harnessed for TES, providing a novel approach for the design of PCMs. Additionally, the phase-change temperature of thermotropic LCs can be finely tuned, which is essential for applications, such as direct steam generation (DSG) in solar thermal power plants. This tunability, together with their inherent liquid state, makes thermotropic LCs highly effective for applications that require repeated thermal cycling and reliable thermal energy management.

Table 1. Comparison of advantages of liquid crystals as phase change materials (LC-PCMs) over traditional solid-liquid PCMs

Aspect	LCPCMs	Solid-liquid PCMs
Phase change state	Liquid state	Solid-to-liquid transitions
Temperature tunability	Can be tuned	Less flexibility in adjusting
Response to temperature changes	Rapid	Slow
Supercooling	Less prone	Possible
Containment	Easy	Require encapsulation
Application range	Wide, including higher temperatures (200-350 °C)	Limited
Thermal conductivity	High, can be engineered	Low
Stability over multiple phase change cycles	Generally stable	May experience degradation or phase separation over time

It is well known that polymers could exhibit phase change behavior with very good physical and chemical properties[37-41]. Apart from pure LCs, LC composites (LCCs) and liquid crystalline polymers (LCPs) and copolymers (LCCPs, a subset of LCPs) have emerged as promising PCMs, offering several advantages over LCs alone. LCCs typically comprise LCs in conjunction with other materials, such as polymers[42,43], micro/nanoparticles[44,45], or encapsulating agents[46,47]. By incorporating LCs into composite structures, their thermal properties are enhanced, and the limitations of using LCs alone can be overcome. The composites exhibited improved thermal conductivity (k), facilitating faster heat transfer during charging, and discharging cycles. Additionally, the composite structure helps stabilize the LC phase, reducing the likelihood of leakage, and enhancing the overall durability of the PCM system[48]. Furthermore, the ability to adjust the phase-change temperature through the addition of nanoparticles or the application of external fields such as electric fields provides greater flexibility in designing thermal-management solutions for specific temperature ranges. Moreover, LCCs can be engineered to have higher latent heat storage (LHS) capacities and better thermal stability than pure LCs, making them more efficient and reliable for long-term TES applications.

LCPs and LCCPs extend the unique properties of LCs when incorporated into polymer matrices, enhancing their mechanical and thermal stability[49-51]. These materials undergo various liquid crystalline phases[52] that can be utilized for TES applications. Moreover, their ability of reversible phase transitions at particular temperatures allows them to absorb and release heat efficiently[53]. Compared with LCs, LCPs and LCCPs offer enhanced mechanical strength, thermal stability, processing and potential for stimuli-responsive behavior; however, they may require more complex synthesis and processing techniques[54,55].

Several review articles on the PCMs and their applications in TES systems are present in the literature[21,22,56-64]. The LCs and their composites are used in different applications including flat panel displays, adaptive lenses and filters, photonics, sensors, biomedicine, and design and architecture which are highlighted in many review articles[65-70]. They show promise as PCMs in TES applications; however, a review focusing exclusively on this topic is lacking. This comprehensive review examines the utilization of LCs and LC polymers (LCPs) as PCMs in TES systems. This study investigated their unique properties and phase-transition mechanisms and analyzes various LC and LCP types, including nematic, smectic, and cholesteric phases, and their potential to enhance energy storage efficiency. Moreover, it explores strategies to improve the k of LCs and LCPs, such as molecular alignment techniques and the incorporation of thermally conductive fillers. Furthermore, the potential applications of LCs and LCPs in TES systems are investigated, particularly in solar TES and DSG. The review concludes with a discussion of the opportunities and challenges associated with employing LCs and LCPs as PCMs for TES applications.

THERMAL ENERGY STORAGE SYSTEMS

Thermal Energy Storage (TES) systems are technologies designed to store thermal energy for subsequent use in heating, cooling, and power generation applications[56,71]. Three primary types of TES systems exist: sensible heat storage (SHS), LHS, and thermochemical heat storage (TCHS) [Figure 2A]. SHS stores thermal energy by increasing or decreasing the temperature of a solid or liquid medium without changing its phase. In contrast, LHS stores energy through PCMs that undergo a change in physical state during the heat storage and release process, allowing for a higher energy storage capacity per unit volume than SHS. TCHS systems store and release thermal energy via reversible chemical reactions, offering the potential for even greater storage capacity than LHS systems.

TES systems possess versatile temperature capabilities, typically spanning from -40 to 700 °C, while offering storage capacities ranging from 10 to 2,250 MJ/m^3. These systems play vital roles in numerous applications such as the integration of renewable energy sources to address the intermittent nature of solar and wind power. For example, a novel approach to generating electricity from concentrated solar power, termed solar thermal electricity via advanced LHS (STEALS), was developed [Figure 2B][72]. This technology harnesses concentrated solar flux to produce high-temperature thermal energy, which is then converted into electricity through thermoelectric generators (TEGs)[73-79]. A key component of STEALS is the use of PCMs for energy storage, which allows the generation of electricity when solar radiation is not available. The modularity of STEALS, with its solid-state TEGs, enables it to be scaled down to smaller kilowatt-range systems, which are more cost-effective than large-scale commercial concentrating solar power (CSP) plants[80]. Other applications include energy storage during low-demand periods, which can be utilized during peak demand times; sector integration to enhance overall energy system efficiency through the utilization of off-peak electricity and waste heat; grid management to alleviate pressure on the power grid and potentially prevent the need for costly upgrades; and seasonal energy storage for preserving summer heat for winter use or winter cold for summer cooling purposes.

Although TES systems present numerous benefits, they encounter challenges, such as restricted application scenarios, relatively immature technology, and efficiency limitations in the thermoelectric conversion process [Table 1]. Despite these obstacles, TES continues to be a promising technology for enhancing energy efficiency and integrating renewable energy sources into power grids.

LCs and LCCs as phase change materials

LCs and LCCs possess remarkable potential as PCMs in TES systems, owing to their exceptional characteristics. Their distinctive properties and mechanisms offer potential enhancements for various applications, particularly in building climate control. Unlike conventional PCMs, which typically undergo solid-liquid transitions, LCs can exhibit mesophases [Figure 1B], intermediate states between solid and liquid states, arising from the interactions (noncovalent and orientation dependent) between the molecules of the condensed phases[81]. These mesophases are formed due to anisotropic geometric shape of the molecule: (1) rod-shaped (a rigid core and a flexible chain); (2) disc-shaped (a flat aromatic core based on benzene triphenylene or truxene); and (3) banana-shaped or bent-core (V-shaped structures incorporating a bent-shaped rigid core) [Figure 3A][65]. Different mesophases provide a range of tunable thermal and optical properties that can be utilized for efficient thermal management. For example, Figure 3B shows transition from nematic phase to isotropic phase in (rod-shaped) LC, 4-cyano-4′-pentylbiphenyl (5CB, molecule shown in Figure 3A), when observed between crossed polarizers using a polarizing optical microscope. With the increase in temperature (T), the 5CB appears into a dark isotropic phase, which returns to nematic phase with the decrease in temperature. Similarly, Figure 3C shows different mesophases (e.g., nematic, smectic and chiral) of LC illustrating the typical defects and textures when observed between crossed polarizers[65].

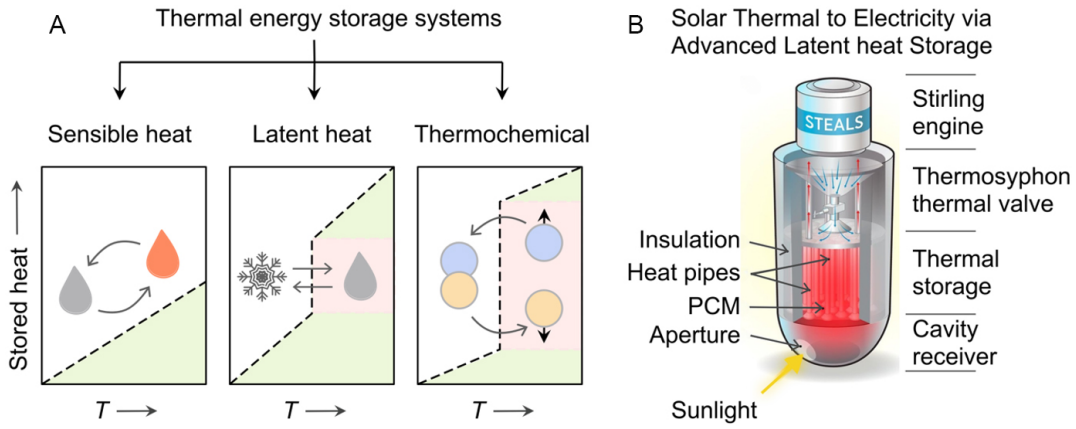

Figure 2. Thermal energy storage (TES) systems. (A) The classification of TES systems with general plots of stored heat *vs.* temperature. (B) Schematic of solar electric conversion via latent heat storage (LHS). Reproduced from ref.[71] Copyright (2018), with permission from Elsevier.

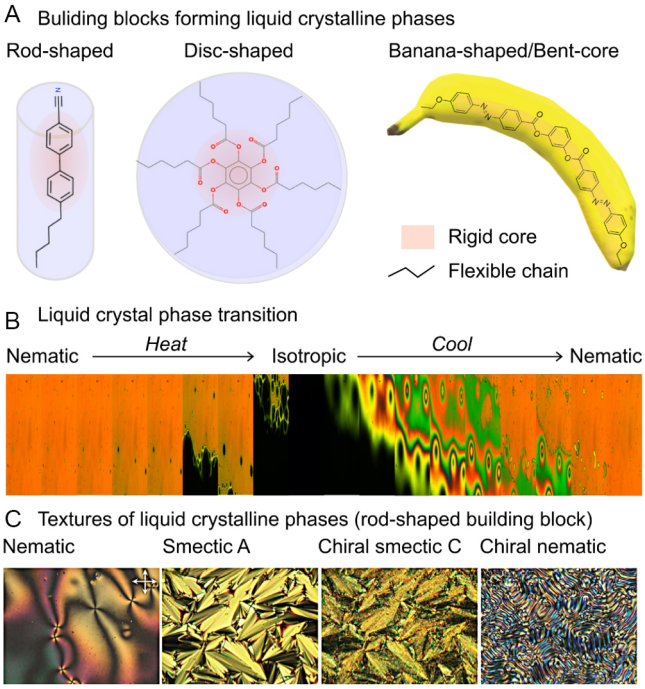

Figure 3. Liquid crystals and their mesophases. (A) Geometrical shapes of the building blocks of LCs that for different phases with temperature; rod-shaped, 4-cyano-4′-pentylbiphenyl (5CB); disc-shaped, benzene-hexa-n-alkanoate derivative; banana-shapes or bent-core, 1,3-phenylene bis(4-(4-ethoxyphenyl) diazenyl) benzoate. Reprinted from ref.[65], with permission from John Wiley and Sons. (B) Nematic to isotropic phase transition in rod-shaped 5CB LC when viewed between crossed polarizers. Snapshots of the video posted on YouTube (https://www.youtube.com/watch?v=yl_YeOf8gJc). (C) Typical phase textures of LC samples prepared on untreated glass slides viewed between crossed polarizers using a polarizing optical microscope. Reprinted from ref.[65] under the terms of the Creative Commons CC BY license.

LCs and LCCs have been used as PCMs for TES applications, owing to their unique thermal and structural properties. For example, polymer-dispersed LCs (PDLC) combined with nanoparticles (e.g., $CaCu_3Ti_4O_{12}$, CCTO) have demonstrated significant advancements in TES applications[82]. These high dielectric constant

(k) LCCs were synthesized using various ratios of polyvinyl chloride (PVC) and polyaniline (PANI), with the incorporation of E7 LC (a mixture of 4-Pentyl-4-cyanobiphenyl - 50.6%; 4-Heptyl-4-cyanobiphenyl - 25.2%; 4-Octyl-4-cyanobiphenyl - 17.8% and 4-Pentyl-4-cyanoterphenyl - 6.4%) and CCTO nanoparticles. The specific composition of PVC/PANI/E7/CCTO (50/50/5/10) exhibited particularly favorable properties for energy storage applications, demonstrating an energy density of 74.66 J/cm^3 and high permittivity values. The alignment properties of E7, in conjunction with the ordering of nematic droplets, enhanced the diffusion of charge carriers within the PDLC nanocomposites, thereby improving their performance.

The anisotropic nature of LCs allows directional heat transfer, potentially enhancing the efficiency of energy storage and release. During transitions from smectic to isotropic phases, LCs can absorb significant latent heat without a corresponding temperature change. This property is particularly advantageous for applications requiring thermal regulation, as it enables LCs to store excess heat during periods of high temperatures and release it when necessary. The specific heat capacity varies across phases. Smectic phases typically exhibit higher specific heat capacities than nematic phases because of their greater molecular organization, which contributes to their enhanced capacity to store thermal energy[83]. Moreover, factors such as the molecular shape and chain length influence the stability and range of mesophases, thereby affecting their thermal properties. For instance, longer alkoxy chains can enhance the range of mesophase stability and improve energy storage capabilities by facilitating improved molecular packing and reducing melting temperatures (T_m)[84]. The interplay between the molecular design and phase behavior of LCs is an attractive candidate for replacing traditional PCMs in specific TES applications, potentially resulting in more efficient and adaptable solutions[85].

LCPs as phase change materials

Functional polymers have been explored for various applications due to the polymeric chains and various functionalities[86-89]. Similar to LCs and LCCs, LCPs exhibit significant potential as PCMs for TES applications, owing to their unique thermal and structural properties. LCPs can be classified into several categories, including main-chain, side-chain, combined main-chain/side-chain, and cross-linked [Figure 4A][49,90]. Main-chain LCPs (MCLCPs) incorporate mesogenic units directly into the polymer backbone, providing high thermal stability and mechanical strength, while forming nematic or smectic phases. In contrast, side-chain LCPs (SCLCPs) feature mesogenic groups attached as side chains to a flexible backbone, allowing for enhanced flexibility and tunability of their properties, which is advantageous for responsive applications. The combined main-chain/side-chain LCPs (MCSCLCPs) can utilize both types of mesogenic units, resulting in unique supramolecular structures with distinct thermal and mechanical properties. Furthermore, cross-linked LCPs are formed by creating covalent bonds between the polymer chains, resulting in a 3D network that enhances thermal stability and mechanical strength while improving the stability of the LC phase. Each type of LCP offers distinct advantages, making it suitable for a wide range of applications in advanced materials, electronics, and responsive devices, with ongoing research exploring novel synthesis methods and applications to enhance their functionality and versatility.

LCPs often exhibit various phase behaviors, making them suitable for advanced applications. For example, a novel bifunctional benzoxazine monomer (BA-ac) containing cholesterol-based mesogens has been used to synthesize cross-linked LCP polybenzoxazine [poly(BA-ac)] [Figure 4B][91]. BA-ac exhibited monotropic smectic C LC behavior, whereas poly(BA-ac) incorporated a smectic C-phase structure. The phase textures of poly(BA-ac) depend on the isothermal curing temperature (T = 220 °C and T = 240 °C) [Figure 4C]. The development of the liquid crystalline arrangement in poly(BA-ac) primarily resulted from the strong tendency of the cholesterol-based mesogen to form LCs and their placement on the side group of the cross-linked network. The liquid crystalline phase of poly(BA-ac) cured at T = 240 °C, disappeared at 274 °C [Figure 4C].

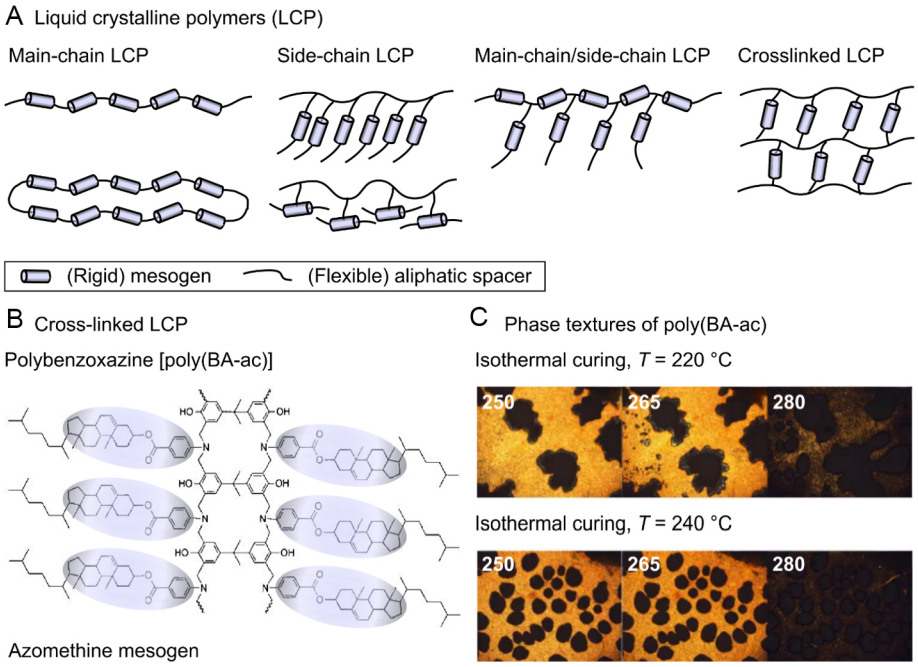

Figure 4. Different categories of liquid crystal polymers (LCP) and their phases. (A) Schematic showing different categories of LCPs. (B) Molecular structure of polybenzoxazine [poly(BA-ac)]. (C) Polarizing optical microscope images of poly(BA-ac) at isothermal curing temperatures of 220 and 240 °C. Reprinted from ref.[91], Copyright (2023), with permission from Elsevier.

Recent advancements have focused on utilizing the unique properties of LCPs, such as their capacity to undergo phase transitions and their responsiveness to light, to enhance their energy storage capabilities. For example, the enhancement of solar thermal fuel using a liquid crystalline block copolymer, poly(ethylene oxide)-block-poly(azobenzene) (PEO-b-PAzo), represents a significant advancement in TES applications[92]. This copolymer effectively integrated a light-inactive PCM, poly(ethylene oxide) (PEO), which facilitated the dual storage of solar energy and latent heat, achieving an energy density increase of approximately 30% compared with traditional materials. The Azo moieties within the LCP enabled the conversion of light energy into thermal energy via photoisomerization with reported efficiencies of up to 85% for converting absorbed light into stored thermal energy. Meanwhile, the PEO block contributed to heat storage through phase transitions with a T_m of ~39 °C and a crystallization temperature (T_c) of 24 °C. The incorporation of a small-molecule PCM, such as sPEO, enhances the energy density of the composite by promoting nanoscale microphase separation (MPS), which has been shown to lower the T_c of sPEO from 24 °C to as low as 38 °C, thereby improving their compatibility and thermal properties. These innovative composites have potential applications in the development of wearable thermal fabrics that can efficiently absorb and store solar energy and release stored energy at various temperatures, even below 30 °C. This versatility renders them suitable candidates for smart textiles and actuators, particularly in scenarios where precise temperature control is essential.

IMPORTANCE OF THERMAL CONDUCTIVITY IN TES AND ITS ENHANCEMENT

Thermal conductivity of phase change materials (PCMs)

k, an ability of the material to conduct the heat, is an important parameter in determining the efficiency of the latent heat TES systems. It influences the heat transfer to and from the PCM during the charging and discharging cycles[93,94]. Generally, *k* of solid-liquid PCMs is low, typically in the range of 0.2-1.0 W/m·K. The low *k* of PCMs degrades the rates of energy discharge to charge in TES systems[94,95]. The overall performance of the TES systems (e.g., faster charge to discharge time) can be improved significantly by

enhancing the k of the PCMs. It was achieved by incorporating different additives (e.g., nanoparticles) into PCMs (e.g., paraffin wax) or impregnating PCMs into metal foams. The enhancement of k (increase in effective k, k_{eff}) can also be achieved by utilizing fins of high k in direct contact with PCMs[95]. In such an arrangement, the number of fins, pitch of the fins, and length of the fin affect the overall performance of TES. The enhancement in k allows efficient temperature distribution within the TES systems and is dependent on the specific application (e.g., building cooling, electronics thermal management, or solar TES) of the TES system[96]. Table 2 shows typical values of phase T_p and k for different solid-liquid PCMs and their composites.

As the mass fraction of nanoparticles increases, the latent heat of the PCM typically decreases[124]. The increase in mass fraction of nanoparticles (e.g., nano-graphite) in PCM (e.g., paraffin) increases k but decreases the latent heat [Figure 5A][125]. While increased k is beneficial, it frequently results in trade-offs in other properties, particularly latent heat capacity[126]. This reduction can be attributed to the lower specific heat of the nanoparticles compared to that of the PCM, and the disruption of molecular forces within the PCM, which lowers the energy required for phase changes. Consequently, while the k improves, the overall energy storage performance may be compromised because of the decreased latent heat capacity. Increasing the filler loading may enhance the k; however, it can also reduce the latent heat capacity if the filler occupies a space that would otherwise be available for the PCM.

To this end, the figure-of-merit (FOM) as a performance metric approach allows for a comprehensive evaluation of multiple properties, including k, latent heat, and T_m, thus facilitating a more holistic understanding of how fillers affect the overall performance[127-129]. The relationship between these properties is nonlinear and varies depending on the specific materials utilized, necessitating a careful balance tailored to the intended application. For instance, applications that require rapid heat transfer may benefit from higher nanoparticle concentrations, whereas those that prioritize energy storage may require lower concentrations to maintain higher latent heat. The FOM for the cooling capacity (FOM_q) is defined as a metric that accounts for the intrinsic material dependencies of the instantaneous rate of heat flux into the PCM matrix[127]. FOM'_q is a normalized version of FOM_q adjusted by the filler weight percentage[127]. It was calculated to provide a more accurate comparison of the performance of different PCM composites by considering the efficiency of the filler material at various loadings. This normalization aids in assessing the contribution of the filler to the overall performance of the composite, thereby facilitating the comparison of materials with different filler loadings. The FOM_q and FOM'_q analyses of the different fillers in the PCM composites provided valuable insights [Figure 5B][127]. High FOM_q values indicate excellent thermal performance (e.g., rapid heat dissipation or absorption, such as thermal management in solar energy storage), whereas high FOM'_q values signify efficient performance at lower filler loadings, rendering the material more economically viable.

Thermal conductivity of liquid crystals

The k of liquid crystals (LCs) varies depending on their phase. In the nematic phase, LCs demonstrate anisotropic k, with higher conductivity along the direction of director alignment than the perpendicular direction [Figure 6A][130]. This anisotropy arises from the ordered arrangement of molecules, which creates more efficient pathways for heat conduction along the director orientation. Figure 6A shows the measured k of 4-n-pentyl-4′-cyanobiphenyl (5CB) with the director-oriented parallel ($k_{||}$) and perpendicular ($k\perp$) to the heat current. $k_{||}$ was considerably larger than $k\perp$ for $T < T_{NI} = 35.17$ °C.

Compared to nematic (N) phase where molecules share a common orientation but no positional order, the smectic [Smectic A (SmA)] phase exhibits higher degree of molecular order characterized by layered

Table 2. Thermal conductivities and phase transition temperatures of different solid-liquid phase change materials (PCMs) used in thermal energy storage. The comparison of the effective thermal conductivities of paraffin wax PCM with different types of additives

Sr. No.	Material	T_p (°C)	k (W/m·K)	Ref.	Additive	(%w/w)	k_{eff} (%)	Ref.
1	Paraffin wax	32	0.24	[97,98]	SiO_2	0.5	7.86	[99]
2	Caprylic acid	16	0.15	[100,101]	Biochar particles	5	27.3	[102]
3	Capric acid	32	0.15	[100,103]	MWCNT	0.5	32.39	[99]
4	Palmitic acid	57.8	0.22	[104,105]	MWCNT + SiO_2	0.5 + 0.5	40.3	[99]
5	n-Octadecane	28	0.28	[106,107]	MWCNT + SiO_2	1 + 1	46.76	[99]
6	1-Dodecanol	26	0.16	[108]	Ag particles	2	78	[109]
7	Polyglycol E600	22	0.18	[110]	TiO_2	1.5	94	[111]
8	Propyl palmitate	10	0.16	[108,112]	Graphene	10	200	[113]
9	$Na_2HPO_4{\cdot}12H_2O$ (Sodium phosphate dodecahydrate)	36	0.47	[58,114]	Ni foam	-	658	[115]
10	$Na_2SO_4{\cdot}10H_2O$ (Sodium sulfate decahydrate)	32	0.50	[116,117]	xGnP	10	1,080	[113]
11	$Na_2CO_3{\cdot}10H_2O$ (Sodium carbonate decahydrate)	36	0.45	[118]	Diamond foam	-	2,580	[119]
12	$Na_2S_2O_3{\cdot}5H_2O$ (Sodium thiosulfate pentahydrate)	48	0.50	[118]	Cu Foam	-	4,500	[115]
13	$CaCl_2{\cdot}6H_2O$ (Calcium chloride hexahydrate)	29	0.54	[120]	Carbon fiber sheet	17.44	4,670	[121]
14	$Mg(NO_3)_2{\cdot}6H_2O$ (Magnesium nitrate hexahydrate)	89	0.41	[120,122]				
15	$Ba(OH)_2{\cdot}8H_2O$ (Barium hydroxide octahydrate)	78	0.65	[120]				
16	$CH_3COONa{\cdot}3H_2O$ (Sodium acetate trihydrate)	58	0.61	[123]				

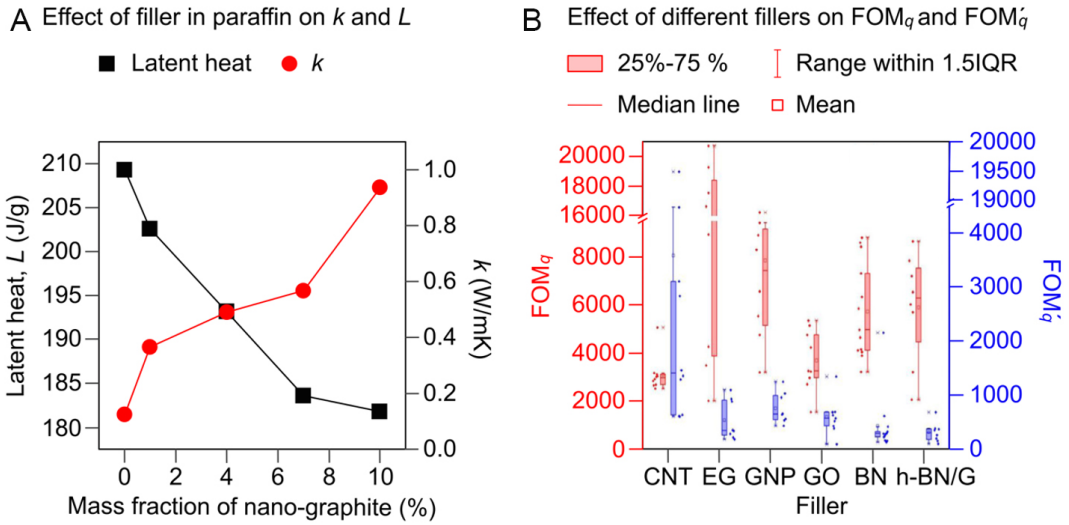

Figure 5. Effect of filler on thermal conductivity and latent heat of phase change materials. (A) A plot of latent heat and thermal conductivity *vs.* mass fraction of nano-graphite in paraffin. Reprinted from ref.[125], Copyright (2013), with permission from Elsevier. (B) Effect of different types of fillers on the overall figure of merit (FOM_q and FOM'_q) metrics. Reprinted from ref.[127] under the terms of the Creative Commons CC BY license.

structures[133], which can further enhance k[131]. Figure 6B shows measured k of as a function of T for homeotropic and planar 4-n-nonyl-4′-cyanobiphenyl (9CB)[131]. In the homeotropic ($k_\perp$) and planar ($k_\parallel$)

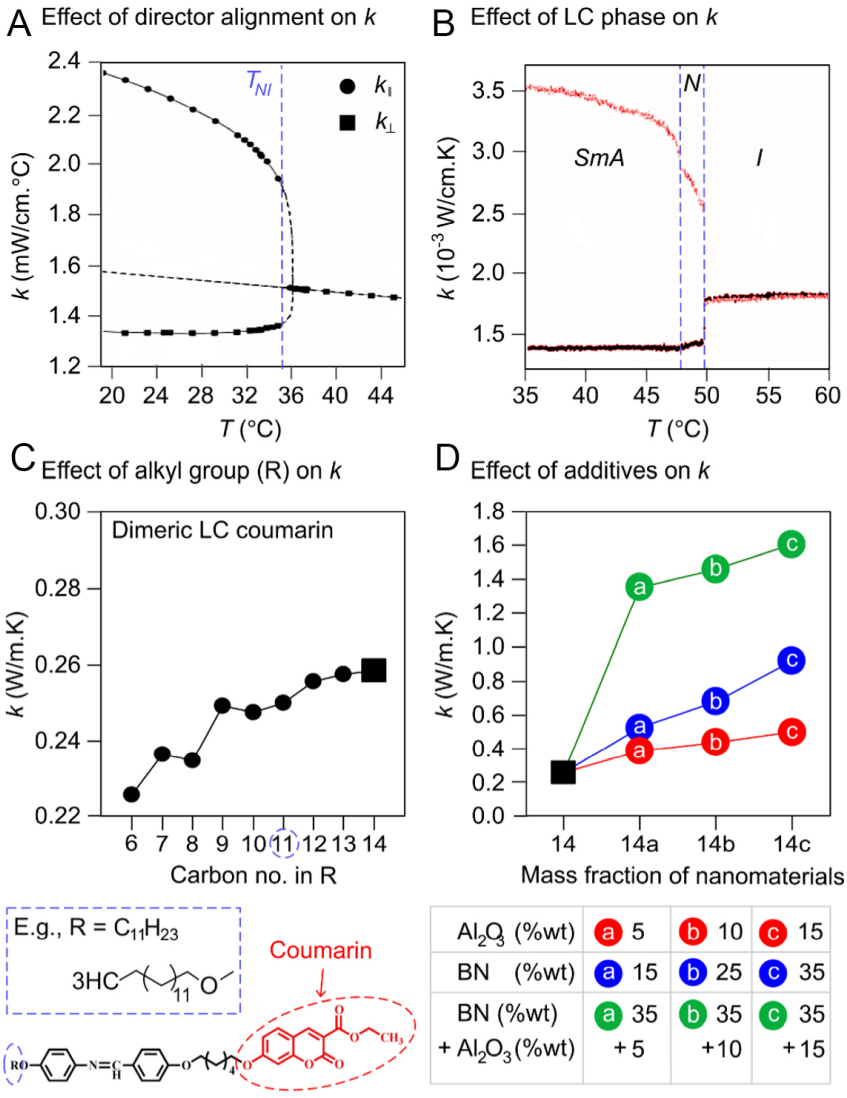

Figure 6. Dependence of phases of liquid crystals and additives (e.g., nanomaterials) in liquid crystals on the thermal conductivity. Thermal conductivity as a function of temperature for homeotropic ($k_{\perp}$, red dots) and planar ($k_{||}$, black dots) configurations of the (A) 5CB (the vertical line is the nematic-to-isotropic transition line, T_{NI} = 35.17 °C), and (B) 9CB molecules. (A) Reproduced with permission from ref.[130]. Copyright (1994) by the American Chemical Society. (B) Reproduced with permission from ref.[131]. Copyright (1998) by the American Chemical Society. (C) Thermal conductivity of dimeric coumarin liquid crystals. (D) Thermal conductivity of dimeric coumarin liquid crystal (carbon no. in R = 14) mixed with alumina (Al_2O_3) nanoparticles and boron nitride (BN) nanosheets. Reprinted from ref.[132], Copyright (2023), with permission from Elsevier.

configuration, the 9CB molecules were aligned perpendicular and parallel to the substrate, respectively. $k\perp$ and $k_{||}$ of 9CB vary significantly during phase transitions. During the SmA-N transition, it exhibited higher $k\perp$, remaining relatively constant with a slight increase near the transition due to enhanced molecular alignment facilitating heat transfer. In contrast, $k_{||}$ remained constant with $k_{||} < k\perp$. As 9CB transitioned from N-I transition, $k\perp$ increased just before the transition, reflecting the loss of molecular order and allowing for more isotropic heat conduction. $k_{||}$ also increased during this transition, but the change was less pronounced. $k\perp$ and $k_{||}$ remained relatively constant in the isotropic region as the molecular order was lost. Overall, this behavior underscores the complex relationship between molecular orientation and thermal transport properties in LCs during phase transitions.

The addition of nanoparticles into LCs can significantly alter their properties, including phase transitions, molecular alignment, and electrical, optical, and thermal characteristics[134-136]. The addition of thermally conductive nanomaterials with high *k* can effectively improve *k* of LCs. Many studies have demonstrated the use of nanomaterials (e.g., CdS[137], gold[138], graphene oxide[139], alumina[132,140] nanoparticles, and boron nitride[132] nanosheets) for enhancing the *k* of LCs. For example, dimeric coumarin incorporated nematic phase structures were designed and synthesized[132]. The dimeric liquid crystalline coumarin compounds were synthesized by etherification condensation synthesis between coumarin and various compounds containing hexane as a spacer molecule with different alkyl groups (carbon number increased from 6 to 14) (see inset in Figure 6C). The *k* for these LC compounds increases with their molecular weight from 0.22-0.26 W/m·K [Figure 6C]. The increase in molecular weight led to an increase in crystallinity owing to limited conformability of the molecules. The increased crystalline phases suppressed the phonon scattering by their effective transportation leading to increased *k*. When these compounds were doped with Al_2O_3 nanoparticles (AlNP, size > 50 nm) and BN nanosheets (BNNS, size ~1 mm), the *k* increased linearly with the nanomaterials fraction [Figure 6D]. The addition of 5%w/w of AlNP and 35%w/w of BNNS in the LC compound containing R = $C_{14}H_{29}$ (R14) increased its *k* by ~96% and 355%, respectively, than the intrinsic value of R14. However, a combination of AlNP with BNNS showed excellent *k*; the *k* of BNNS (35%w/w) + AlNP (15%w/w) increased by 619.6% than the intrinsic value of R14. The efficient distribution of AlNPs within the 5i-LCs matrix formed a network that connected the separated BNNS, thereby promoting phonon transport. Moreover, the synergistic effects of various fillers, combined with the high specific energy and ultrathin BNNS with a large surface area, enhanced the *k* of the composite compared to R14 LCs.

Overall, nanoparticles can improve the *k* and heat dissipation capacity of LCs, which may increase their operational temperature range[135]. However, they also have certain disadvantages, such as a decrease in clearing temperature, reduced overall orientational order, and potential deterioration in response time and contrast ratio[136,141-143]. The type, shape, and concentration of nanoparticles play important roles in determining these effects, with metals, metal oxides, and carbon-based nanoparticles each imparting unique changes.

Thermal conductivity of liquid crystal polymers

Liquid crystal polymers (LCPs) are a unique class of materials that possess the properties of LCs and structural characteristics of polymers. One of their key features is their ability to exhibit LC behavior at different temperatures, which can be further enhanced through various processing techniques. These techniques can be used to orient the LCPs and improve their mechanical and thermal properties. The enhancement of *k* in LCPs can be achieved by optimizing several parameters, including the molecular structure, blending with other polymers, incorporation of filler materials, hydrogen bonding, processing conditions, polymerization techniques, and external stimuli. Each of these factors plays a crucial role in optimizing the thermal properties of the LCPs.

Molecular structure

The rigidity of the backbone and the flexibility of the chain play crucial roles in determining the *k* of amorphous polymers[144-147]. The radius of gyration (R_g) is directly affected by these factors, with rigid backbones resulting in larger radii of gyration and extended chain morphologies [Figure 7A-i]. This enhances the *k* by allowing longer thermal transport pathways along the covalent bonds. In contrast, flexible backbones lead to smaller radii of gyration and more disorganized structures, which results in reduced *k* owing to increased phonon scattering and shorter effective transport paths.

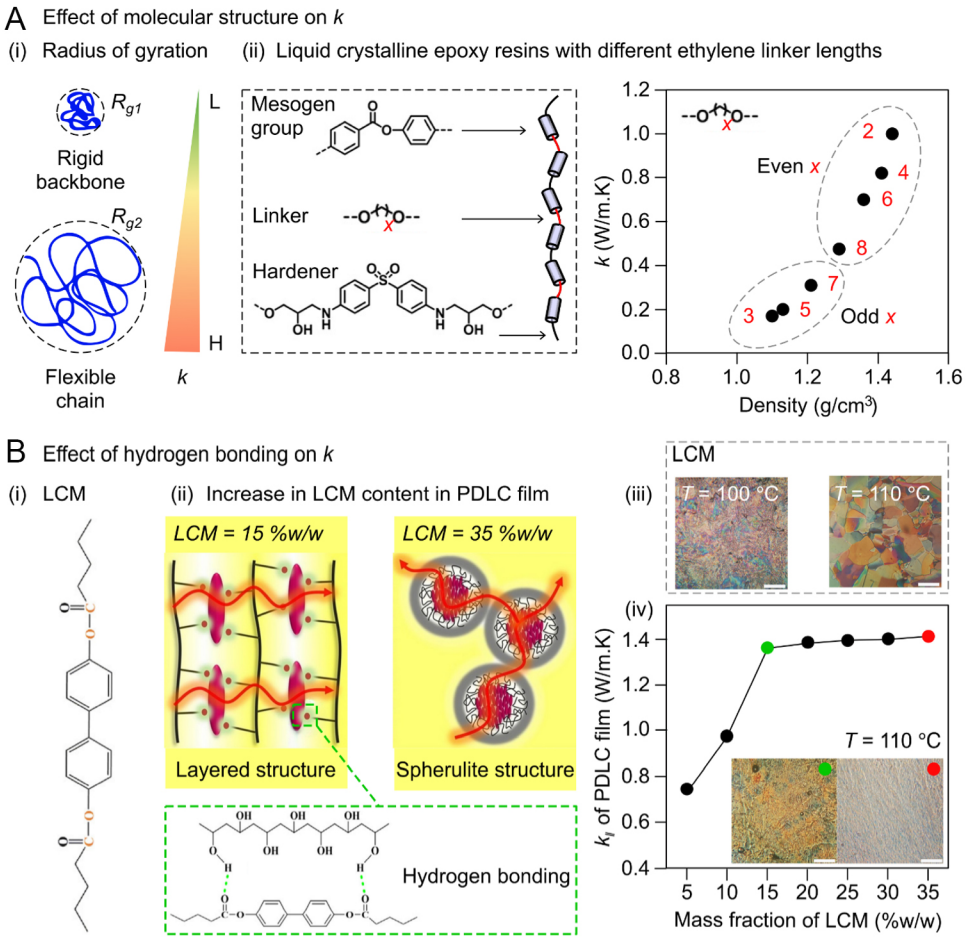

Figure 7. Enhancement of *k* of LCP by controlling molecular structure and by hydrogen bonding. (A-i) Schematic showing effect of chain flexibility and backbone rigidity on the packing of the polymer chain (radius of gyration, R_g). *k* of configuration with larger R_g (R_{g2}) is greater than smaller R_g (R_{g1}) owing to longer thermal transport pathways. (A-ii) Schematic and molecular structures of LC epoxy resins with different ethylene linker lengths cured by mixture of C_x (x = 2-8) diepoxide monomer (mesogen) and diaminodiphenylmethane (DDM). A plot showing thermal conductivity (*k*) as a function of mass density. The values of *k* and density depend on the linker length. Reproduced from ref.[148] under the Creative Commons CC BY-NC-ND License. (B-i) Molecular structure of the liquid crystal monomer (LCM) used in the preparation of polyvinyl alcohol (PVA)-dispersed liquid crystal (PDLC) films. (B-ii) Schematic representation of morphologies of microscopic-ordered arrangements in PDLC films. Layered and spherulite structures are formed owing to hydrogen bond interaction and depending on the concentration of LCM. (B-iii) Polarizing optical microscopy (POM) images of LCM. (B-iv) In-plane thermal conductivity ($k_{||}$) as a function of concentration of LCM in PDLC films. Reprinted from ref.[149], Copyright (2021), with permission from Elsevier.

A significant odd-even effect[150] on the *k* of liquid crystalline epoxy resins (termed C_x/DDM) with different ethylene linker lengths cured by a mixture of C_x diepoxide monomer (x = 2-8) and diaminodiphenylmethane (DDM) was found (inset in Figure 7A-ii)[148]. The epoxy resins with even linker lengths, such as x = 2, 4, 6, and 8, exhibited a liquid crystalline structure and achieved $k \sim 1.0$ W/(m·K), while those with odd lengths, including x = 3, 5, and 7, were amorphous and had lower conductivity at 0.17 W/m·K [Figure 7A-ii]. Additionally, even-length resins demonstrated a higher mass density, reaching up to 1.44 g/cm^3. The even-length linkers enhanced the molecular ordering and facilitated better packing of the mesogen groups, which contributed to their enhanced thermal performance. In contrast, odd-length linkers resulted in amorphous structures that lacked this ordered arrangement, significantly reducing their *k* owing to poorer molecular interactions and packing efficiency. Similar to LCs, the *k* of LCPs can be further enhanced by doping with nanoparticles, such as AlNPs[151].

Hydrogen bonding

The presence of hydrogen bonds within the components can potentially enhance k by creating additional channels for heat transfer[152-154]. The relationship between the liquid crystalline textures and hydrogen bonds resulted in improved thermal properties, as these bonds aided energy transfer between adjacent polymer chains[149,155]. For example, the enhancement of k in PDLC films [Figure 7B], particularly those composed of polyvinyl alcohol (PVA) and LC monomers (LCMs) [Figure 7B-i], can be attributed to the synergistic effects of liquid crystalline textures and hydrogen bonding interactions[149]. The ordered stacking of LCM within the PVA matrix facilitated the formation of microscopic-ordered structures that promoted efficient phonon transport, significantly increasing $k_{||}$ to 1.41 W/m·K at a fraction of 35%w/w, which was approximately 10.8 times greater than that of the neat [Figure 7B-iii and B-iv]. The role of LCM concentration was crucial in determining the morphological characteristics of the PDLC films. At lower concentrations, LCM promoted the formation of layered structures, whereas at higher concentrations, it promoted the development of spherulite structures [Figure 7B-ii]. This is visually represented in Figure 7B-iii, which shows a distinct layered morphology at lower LCM fractions and the transition to spherulite structures at higher LCM concentrations. Concurrently, hydrogen bonding between the LCM and PVA chains fostered the development of interpenetrating layered networks, enhancing interfacial compatibility and interchain coupling. This interaction not only stabilizes the molecular arrangement but also reduces phonon scattering, which is a common challenge in disordered polymer systems. Collectively, these structural improvements led to a more organized molecular architecture that markedly enhanced the thermal conductivities of the polymer films.

Processing conditions

The effects of various processing techniques and conditions on the thermal properties of amorphous polymers, LCPs, and crystalline or semicrystalline polymers are significant. Key factors include the alignment of polymer chains, which can be enhanced by shear forces during extrusion, gel spinning, and simple shear deformation[156-160]. These techniques help reduce phonon scattering, thereby improving heat conduction. Moreover, processing conditions such as temperature and shear rate can influence the crystallinity and molecular orientation of polymers, ultimately optimizing their thermal performance.

Advances in digital fabrication, particularly 3D printing, have revolutionized manufacturing across various fields including biotechnology and materials science. Extrusion-based 3D printing [e.g., fused deposition modeling (FDM) and direct ink writing (DIW)[161]] allows for the creation of complex 3D objects by depositing materials layer-by-layer. As the printing ink is forced through the nozzle, it experiences shear and elongational flows, which can align the polymer chains in the direction of the flow[162]. One of the key advancements in 3D printing is the ability to control the orientation of molecules during the printing process, which can significantly enhance the properties of the printed objects[163].

The 3D printing LCPs primarily utilized FDM to form complex geometries [Figure 8A-i][164-167]. During printing, the unique properties of LCPs enable the nematic alignment of polymer chains [Figure 8A-ii], resulting in highly ordered domains that enhance thermal and gas-barrier properties and mechanical strength. In addition, the nozzle diameter and the extrusion rate significantly influenced the flow behavior and molecular orientation of the LCPs during 3D printing[166]. Altering the extrusion rate alters the dimensions of the printed filament at the exit[168-171]. The ratio of the line width to the nozzle diameter influenced the distribution of the nematic domains, which remained parallel to the travel direction when below unity. In contrast, when the ratio exceeded unity, the transverse flow component caused a segment of domains to solidify at an angle in the longitudinal direction. Manipulating the linewidth permits the creation of a controlled stiffness gradient within a single line. This interplay between shear and elongational

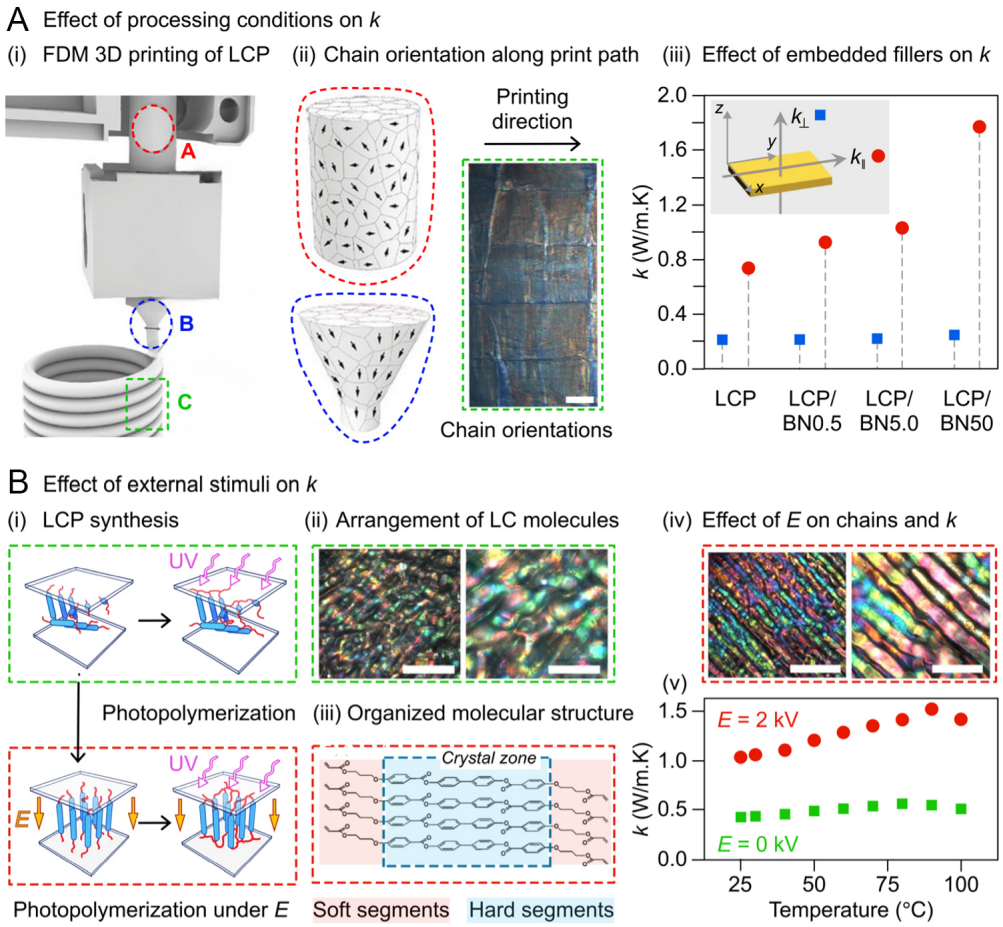

Figure 8. Enhancement of *k* of LCP by controlled processing conditions and by external stimuli. (A) Schematic diagram of (A-i) FDM 3D printing process of a vacuum-tight LCP and print path and, (A-ii) orientations of polymer chain within the printed filament, before and after extrusion. (A-iii) A plot of anisotropic *k* as a function of concentration of BN fillers in the printed LCP composites. Reprinted from ref.[164] under the Creative Commons CC-BY-NC license, and ref.[165], Copyright (2021), with permission from Elsevier. (B-i) The schematic showing alignment of monomers. (B-ii) Images of polarising microscope of LCP under *E* = 2 kV. First image scale = 800 mm, and second image scale = 400 mm. (B-iii) Molecular structure of crystal monomer under electric field. (B-iv) Images of polarising microscope of LCP under *E* = 0 kV. First image scale = 800 mm, and second image scale = 400 mm. (B-v) A plot showing thermal conductivity of the samples with increase in temperature. Reprinted from ref.[172] under the Creative Commons Attribution 4.0 International License.

flow results in variations in mechanical properties, such as stiffness, depending on the nozzle size and the extrusion rate used during the printing process.

It is well known that the matrix structure will be important to hold various fillers for specific performance[172-176]. Incorporating fillers such as hexagonal BN into printing ink has a significant impact on the thermal properties of 3D printed LCP composites (LCPCs)[165]. The degree of orientation of BN within the LCP matrix is influenced by its lateral size. Larger BN particles displayed a higher degree of orientation, contributing to improved *k*. The processing conditions that promote the orderly arrangement of these fillers are critical to achieving high thermal performance in the final composite material. The in-plane *k* ($k_{||}$) of the neat LCP was initially measured at 0.74 W/m·K and increased to 1.77 W/m·K with the addition of 20%w/w of BN [Figure 8A-iii]. This enhancement is attributed to the well-ordered arrangement of both the LCP and BN, which creates continuous thermal pathways, facilitating better heat transfer. It should be noted that incorporating 20%w/w BN into the LCPs slightly reduced the tensile strength. This reduction is likely due to

the introduction of defects during 3D printing by the smaller BN particles, necessitating careful consideration of the particle size to maintain the mechanical properties.

External stimuli

External stimuli, such as electric fields[177-179], magnetic fields[180,181], light exposure[182,183], and humidity[184,185], can significantly influence the k of LCPs[186]. For example, applying an electric field can align molecular chains, enhancing k by creating more efficient pathways for heat transfer. Similarly, exposure to light can induce phase transitions that alter the thermal properties. The absorption of moisture can also affect chain mobility, potentially enhancing k.

It was demonstrated that by applying an external electric field (E = 2 kV) to LC acrylic acid monomers, LC molecules were effectively aligned during the photopolymerization process, leading to the formation of a crystal region [Figure 8B-i and B-ii][172]. The LC consists of a hard segment comprising conjugated aromatic structures, which tend to form periodic arrangements owing to the assistance of p-p interactions [Figure 8B-iii]. Initially, the LCMs separated into distinct regions with defined boundaries [Figure 8B-ii], which collectively formed large, connected areas, indicating the presence of an organized molecular structure under an electric field of 2 kV [Figure 8B-iv]. This alignment resulted in an LCP with a high intrinsic k of 1.02 W/m·K, which was a significant improvement compared to typical values for unaligned polymers, which were generally k < 0.5 W/m·K. The increase in temperature was accompanied by a change in k, which first increased before subsequently decreasing, indicating the occurrence of phase transition [Figure 8B-v].

Overall, the k of LCPs can be effectively enhanced by carefully manipulating these parameters, making them suitable for a wide range of applications in electronics, thermal management, and advanced materials. Understanding the interplay between these factors is crucial for optimizing the performance of LCPs in practical applications.

LIQUID CRYSTAL-BASED THERMAL ENERGY STORAGE APPLICATIONS

Solar thermal energy storage system

In recent developments in solid-state solar thermal fuels (SSTFs), a novel approach of storing solar energy as chemical potential energy using discotic nematic LCs has been explored, focusing on compounds incorporating tetra-ortho-fluoro/chloro-azobenzene arms within a triphenylene-based LC framework [Figure 9A-i][187]. These innovative compounds are designed to efficiently absorb solar energy and subsequently release it as heat, even under sub-zero temperature conditions. Notably, the ability of these compounds to undergo photoisomerization in the visible light spectrum enhances their practicality, distinguishing them from existing systems that often depend on ultraviolet light or additional heating. The synthesized compounds exhibited remarkable photocyclability and photostability, achieving charging efficiencies of up to 77% under sunlight with and without a bandpass filter and 62.4% without it, underscoring their potential for effective energy storage applications.

The experimental results further clarified the thermal isomerization properties of these compounds, with compound 1 displaying a half-life of approximately 7.19 days and compound 2 with a half-life of about 3.32 days at room temperature. Upon discharging, the systems can achieve temperature increases of up to 6.5 °C at room temperature and 29.5 °C at sub-zero temperatures (around -6 to -7 °C) [Figure 9A-ii]. These findings indicate that these compounds can efficiently release stored energy, making them suitable for practical applications in solar TES. The *trans*-azobenzene configuration demonstrates greater stability than its *cis* counterpart, thus requiring more energy for conversion to the less stable *cis* form. This differential

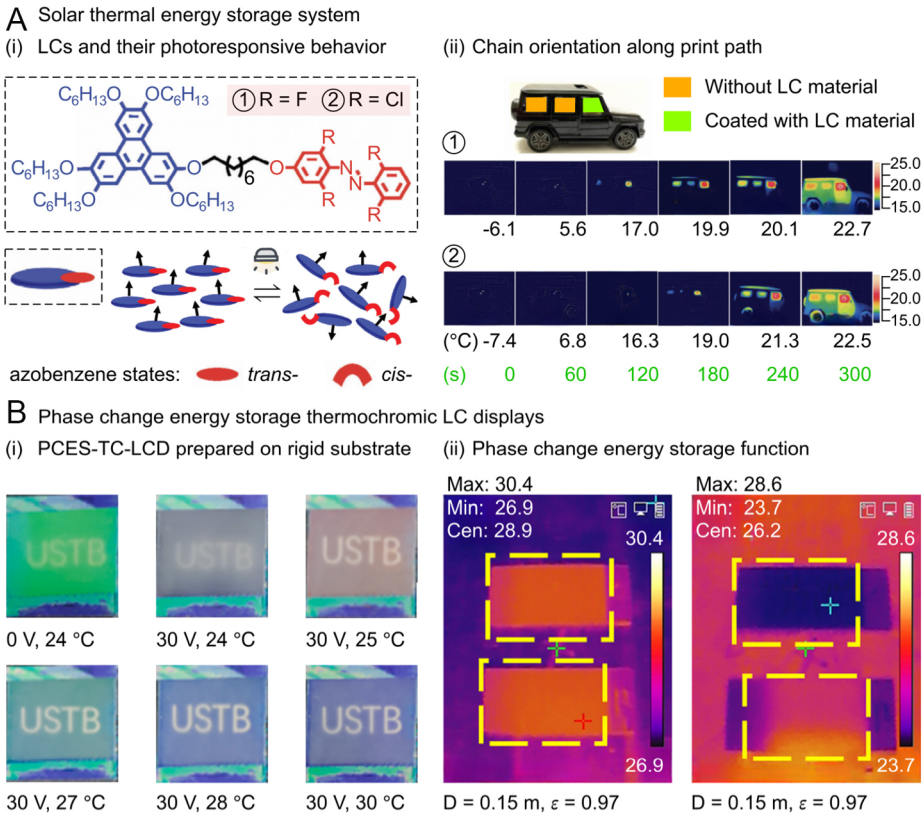

Figure 9. LCs and LCPs as PCMs for TES applications. (A) Solar energy thermal storage system. (A-i) Schematic showing design of LC molecules in the study of solid-state solar thermal fuels (SSTF) and their photo-responsive behavior. (A-ii) IR thermal camera images of heat release from *cis*-rich films of ① R = F, and ② R = Cl coated on the window of a mini car under 430 nm irradiation for *cis* to *trans* conversion, at sub-zero temperature. Reprinted from ref.[187], with permission from John Wiley and Sons. (B) Phase change energy storage thermochromic LC displays. (B-i) Optical images showing phase change energy storage thermochromic liquid crystal display (PCES-TC-LCD) prepared on rigid substrates at different voltages and temperatures. (B-ii) Infrared thermography images showing energy storage and energy release. Reprinted from ref.[42], Copyright (2023), with permission from Elsevier.

stability influences the quantity of energy stored during the phase transitions, enabling *trans*-azobenzene to accumulate higher latent heat. Conversely, the *cis* configuration, which is characterized by lower T_m and T_c, can release energy at reduced temperatures, rendering it more efficient in thermal applications. Overall, this research highlights the potential of discotic nematic LCs to provide a promising solution for solar energy storage, extending the operational capabilities of SSTFs in colder climates and contributing significantly to the advancement of sustainable energy technologies. Currently, sustainable materials and technologies are being extensively studied to achieve a sustainable world[188-193].

Direct steam generation

Application of thermotropic LCs as PCMs for TES in DSG solar thermal power plants has been investigated[24,83,194]. Traditional inorganic PCMs, such as $NaNO_3$ and KNO_3, exhibit low k and variable discharge power, thereby reducing the efficiency of the existing TES. It was proposed that by utilizing LCs that can undergo multiple phase transitions and facilitate energy exchange through convection rather than conduction, a more efficient and adaptable storage solution can be obtained. This approach is aimed at improving the thermal management of DSG systems and enhancing the overall energy yield and dispatchability of solar power plants.

Several types of LCs, including N,N′n-dialkanoyl 2,3,5,6-tetramethylbenzene-1,4-diamines (n = 6, 7, 8, 9, 10, 11) and 4-(4-n-alkyloxyphenyliminomethyl) benzoic acids (n = 6, 7, 8, 9, 10, 12), which exhibited phase-change enthalpies, comparable to that of conventional inorganic salts, were investigated. It was demonstrated that a two-tank configuration utilizing LCs could maintain a constant discharge power over time, addressing a significant drawback of the current storage technologies. This capability is particularly important for DSG systems, in which a stable output is essential for operational efficiency.

Calculations for different plant sizes (50 and 100 MW) and various storage capacities (2, 4, 6, and 7.5 h) indicated that LC-based systems could provide effective energy storage solutions with improved performance metrics. For example, a 50 MW plant with a 4-h storage capacity could achieve a more consistent power output compared to traditional systems, enhancing the overall reliability of the energy supply. Although further experimental validation is necessary, the promising results advocate the potential of LCs to enhance TES in solar thermal applications, ultimately contributing to more efficient and cost-effective renewable energy systems.

Phase change energy storage thermochromic LC displays

The development of phase-change energy storage thermochromic LC displays (PCES-TC-LCDs) represented a significant advancement in the integration of thermochromic LCs with phase-change energy storage microcapsules (PCESM)[42]. This innovative display technology features a stable bilayer structure, wherein the lower layer consists of a thermochromic LC layer produced using DYE1001 and the upper layer is a polymer-stabilized LC (PSLC) film obtained through polymerization-induced phase separation. The incorporation of PCESM enables the display to effectively absorb and release heat, enhance energy efficiency, and maintain the color change for extended periods. Notably, the PCES-TC-LCD achieved an improvement in the contrast ratio, with values reaching up to 5.2, while maintaining a lower transmittance of approximately 30% under specific conditions. This study emphasizes the potential of PCES-TC-LCDs in energy-saving applications, particularly in environments where temperature modulation is crucial.

The PCES-TC-LCD demonstrated the capability to effectively reflect primary colors and switch optical states rapidly under electric fields, achieving color changes at temperatures ranging from 24 to 30 °C [Figure 9B-i]. The phase change process facilitated by the temperature field allowed the display to store a significant amount of energy, which could be spontaneously released upon removal of the external field, thereby maintaining the film temperature at the phase-change temperature [Figure 9B-ii]. Additionally, the PCESM exhibited a TES capacity that enabled the display to maintain its color change for extended periods with sensitivity to thermal color changes of less than 1 °C. These results underscore the potential of PCES-TC-LCDs for enhancing the energy efficiency and thermal management in various applications.

Table 3 summarizes LCs and LC-based materials that have been explored or have potential for use as PCMs owing to their thermal properties and phase transition behaviors.

CRITICAL PARAMETERS FOR DESIGNING LC-PCM-BASED SYSTEMS

Several key factors must be addressed in the development of LC-PCM-based systems to achieve optimal functionality and performance. First, the thermal characteristics, including the temperature range for phase transitions, latent heat capacity, and k, are essential for efficient energy storage and transfer. Second, the LC mesophase type (nematic, smectic, or cholesteric), order parameter, birefringence, and dielectric anisotropy play crucial roles in both the thermal and optical performance, particularly in applications requiring precise light control or responsiveness to external fields. Third, material durability, including resistance to chemical, thermal, and photodegradation across multiple cycles, is vital. Fourth, mechanical properties such as

Table 3. A list of LCs and LC-based materials that are explored or have potential for use as PCMs

Category	Material name
Thermotropic LCs	4-Cyano-4'-pentylbiphenyl (5CB)
	4-Octyl-4'-cyanobiphenyl (8CB)
	Cholesteryl derivatives (e.g., Cholesteryl Oleate)
	Eutectic LC mixtures (e.g., E7, BL006)
Ionic LCs	Imidazolium-based LCs
	Phosphonium-based LCs
LC-Polymer composites	Polymer-dispersed LCs (PDLCs)
	LC elastomers (LCEs)
LC-Enhanced PCMs	LC-paraffin composites
	LC-inorganic salt hydrates
Photo-responsive LCs	Azobenzene-based LCs
	Spiropyran-modified LCs
LC Nanocomposites	LC-carbon nanotube (CNT) composites
	$CuInS_2$/ZnS quantum dots-dispersed LCs

encapsulation strength and elasticity ensure resilience under operational stress. Fifth, flexibility to external factors, including environmental conditions and responsiveness to electric or magnetic fields, further enhances the system performance. Finally, integration with supporting systems requires compatibility with host matrices and optimized interfacial properties, while scalability, cost-effectiveness, and sustainability are crucial for economic and environmental feasibility. By addressing these interrelated factors, LC-PCMs can be effectively customized for use in thermal management, energy storage, and smart material applications.

CONCLUSIONS

This review has highlighted the significant potential of LCs as PCMs in the realm of TES. The unique properties of LCs, including their tunable phase transitions, high latent heat, and favorable k, position them as promising candidates for enhancing energy storage efficiency. By examining various types of LCs - such as nematic, smectic, and cholesteric phases - we have illustrated their distinct roles in improving TES systems.

The mechanisms underlying LC phase transitions and their impact on energy storage efficiency have been thoroughly discussed, alongside strategies to enhance the thermal conductivities of LCPs. Techniques such as embedding LC units within molecular structures, aligning polymer chains through external fields, and incorporating thermally conductive fillers have shown promise in optimizing thermal performance.

Despite the advancements, challenges remain regarding the scalability, cost-effectiveness, and long-term stability of LC-based PCMs. Addressing these issues is crucial for the practical application of these materials in real-world energy systems. Future research should focus on overcoming these barriers while exploring new formulations and applications of LCs in TES.

In conclusion, this review synthesizes current knowledge and identifies gaps in the literature, providing a valuable resource for researchers and engineers. The insights gained from this work can guide the development of advanced TES technologies, ultimately contributing to sustainable energy solutions and reducing reliance on fossil fuels. As the demand for efficient energy storage continues to grow, the innovative use of LCs may play a pivotal role in shaping the future of energy management.

FUTURE OUTLOOK AND CHALLENGES

LCs, LCCs, and LCPs are emerging as promising materials for TES applications due to their unique phase transition properties and tunable thermal characteristics. Research indicates that LCs can effectively store and release thermal energy through phase changes, which can be optimized for higher energy densities. The integration of environmentally friendly materials, such as ionic liquids and bio-based compounds, into LCs and LCPs is gaining traction, enhancing thermal stability and reducing environmental impact. The development of composite microencapsulated PCMs (MPCMs) allows for better control over thermal properties and improved stability, making them suitable for multi-temperature applications. The versatility of LCs extends to applications in smart textiles, thermal regulation in buildings, and electronic devices, driven by their ability to undergo rapid phase transitions in response to temperature changes. Machine learning (ML) approaches are increasingly being utilized to design LCs[195] with enhanced *k*, addressing the limitations of traditional empirical methods[196]. Recent studies have developed ML models that can predict the formation of liquid crystalline states with over 96% accuracy based on the compositional and structural characteristics of polymers. These models enable the identification of promising chemical structures for liquid crystalline polyimides, leading to the synthesis of polymers with thermal conductivities ranging from 0.722 to 1.26 W/m·K.

In addition to LCs, LC-PCM and LCP-PCM composites are gaining interest because of their effective TES capabilities[197,198]. For example, these composites integrate the advantageous thermal properties of paraffin wax with the structural benefits of LCPs, resulting in enhanced *k* and improved phase change behavior. One of the primary benefits is the enhanced shape stability provided by the 3D network of the LCPs, which effectively encapsulates paraffin[197]. This structural integrity allows the composite to maintain a high concentration of paraffin (~94%wt) without leakage during phase transitions, even at elevated temperatures. While LCs and their derivatives hold substantial promise for TES applications, several challenges must be addressed. Maintaining thermal stability under operational conditions remains a challenge, and research is ongoing to improve the thermal stability of these materials to prevent degradation over time. The production of high-quality LCs and their composites can be expensive and complex, which may limit their widespread adoption in commercial applications. There is a need for standardized testing methods to evaluate the performance of LCs and LCPs in TES applications, including understanding their thermal properties, phase transition behaviors, and long-term performance under varying conditions. Incorporating LCs and their composites into existing thermal energy systems poses technical challenges, including compatibility with current materials and systems used in energy storage technologies. The integration of ML techniques extends beyond mere prediction; it encompasses high-throughput molecular dynamics (MD) simulations to explore *k* of polymers[199,200]. For instance, studies have utilized various ML algorithms, including random forests, to analyze self-assembled structures and phase transitions in liquid crystalline systems[201,202]. This approach allows for the rapid screening of materials, identifying candidates with desirable thermal properties. Moreover, advancements in ML methodologies, such as convolutional neural networks, have demonstrated the capability to predict thermal transport properties directly from optical images of LC textures, enhancing the understanding of mesophase transitions and their implications for *k*. These innovations position ML as a powerful tool in the design and optimization of LCs for TES applications.

DECLARATIONS

Author's contributions

Conducted the literature survey and prepared the manuscript: Karyappa, R.; Lee Joo Cheng, J.
Supervised and guided the academic aspects of this work: Xu, J.; Zhu, Q.

Revised the logic, grammar, and professionalism of the manuscript: Lixuan Ho, C.; Wang, S.; Thitsartarn, W.; Kong, J.; Kai, D.; Tan, B. H.; Wang, P.; Qu, Z.; Loh, X. J.; Xu, J.; Zhu, Q.

Availability of data and materials
Not applicable.

Financial support and sponsorship
This work was supported by the National Research Foundation (NRF) Singapore under its Low-Carbon Energy Research (Grant Reference No. U2305D4001).

Conflicts of Interest
All authors declare that there are no conflicts of interest.

Ethical approval and consent to participate
Not applicable.

Consent for publication
Not applicable.

Copyright
© The Author(s) 2025.

REFERENCES
1. Mao, Y.; Miyazaki, T.; Sakai, K.; Gong, J.; Zhu, M.; Ito, H. A 3D printable thermal energy storage crystalline gel using mask-projection stereolithography. *Polymers* **2018**, *10*, 1117. DOI PubMed PMC
2. Salyan, S.; Suresh, S. Liquid metal gallium laden organic phase change material for energy storage: an experimental study. *Int. J. Hydrogen. Energy.* **2018**, *43*, 2469-83. DOI
3. Krašna, M.; Klemenčič, E.; Kutnjak, Z.; Kralj, S. Phase-changing materials for thermal stabilization and thermal transport. *Energy* **2018**, *162*, 554-63. DOI
4. Zhang, H.; Sun, Q.; Yuan, Y.; Cao, X. Porosity reduction of polyethylene glycol phase change materials by using nanoscale thermal-energy-conducting medium during crystallization process. *J. Appl. Polym. Sci.* **2017**, *134*, 45446. DOI
5. Zhu, Q.; Ong, P. J.; Goh, S. H. A.; et al. Recent advances in graphene-based phase change composites for thermal energy storage and management. *Nano. Mater. Sci.* **2024**, *6*, 115-38. DOI
6. Wu, W. Y.; Yeo, G. M. D.; Wang, S.; Liu, Z.; Loh, X. J.; Zhu, Q. Recent progress in polyethylene-enhanced organic phase change composite materials for energy management. *Chem. Asian. J.* **2023**, *18*, e202300391. DOI
7. Wu, W.; Yeap, I. S. R.; Wang, S.; et al. Advancements in sustainable phase change materials: valorizing waste for eco-friendly applications. *Mater. Today. Chem.* **2024**, *39*, 102163. DOI
8. Lee, J. J. C.; Hayat, N. N. A.; Soo, X. Y. D.; et al. Upcycling of PET plastics into diethyl terephthalate for applications as phase change materials in energy harvesting. *J. Energy. Storage.* **2023**, *73*, 109084. DOI
9. Prieto, C.; Cabeza, L. F.; Pavón-moreno, M. C.; Palomo, E. Thermal energy storage for direct steam generation concentrating solar power plants: concept and materials selection. *J. Energy. Storage.* **2024**, *83*, 110618. DOI
10. Kumar, A.; Sahoo, U.; Rathod, B. K. J. Solar thermal power plant with thermal energy storage; 2021. pp. 31-80. DOI
11. Ismail, K.; Henríquez, J. Thermally effective windows with moving phase change material curtains. *Appl. Therm. Eng.* **2001**, *21*, 1909-23. DOI
12. Zhu, N.; Ma, Z.; Wang, S. Dynamic characteristics and energy performance of buildings using phase change materials: a review. *Energy. Convers. Manag.* **2009**, *50*, 3169-81. DOI
13. Ong, P. J.; Lum, Y. Y.; Soo, X. Y. D.; et al. Integration of phase change material and thermal insulation material as a passive strategy for building cooling in the tropics. *Constr. Build. Mater.* **2023**, *386*, 131583. DOI
14. Bui, V.; Liu, H.; Low, Y.; et al. Evaluation of building glass performance metrics for the tropical climate. *Energy. Build.* **2017**, *157*, 195-203. DOI
15. Png, Z. M.; Soo, X. Y. D.; Chua, M. H.; Ong, P. J.; Xu, J.; Zhu, Q. Triazine derivatives as organic phase change materials with inherently low flammability. *J. Mater. Chem. A.* **2022**, *10*, 3633-41. DOI
16. Alawadhi, E. M. 10 - The design, properties, and performance of concrete masonry blocks with phase change materials. In: Eco-Efficient Masonry Bricks and Blocks. 2015, Elsevier. p. 231-48. DOI

17. Roy, U.; Pant, H. K. Chapter 9 - Current progress in heat exchangers with phase change materials (PCMs): a comprehensive investigation. In: Advanced Analytic and Control Techniques for Thermal Systems with Heat Exchangers. Elsevier; 2020. pp. 219-30. DOI
18. Şahan, N.; Fois, M.; Paksoy, H. Improving thermal conductivity phase change materials-a study of paraffin nanomagnetite composites. *Solar. Energy. Mater. Solar. Cells.* **2015**, *137*, 61-7. DOI
19. Tebaldi, M. L.; Belardi, R. M.; Montoro, S. R. Chapter 8 - Polymers with nano-encapsulated functional polymers: encapsulated phase change materials. In: Design and Applications of Nanostructured Polymer Blends and Nanocomposite Systems; 2016, pp. 155-69. DOI
20. Hameed, G.; Ghafoor, M. A.; Yousaf, M.; et al. Low temperature phase change materials for thermal energy storage: Current status and computational perspectives. *Sustain. Energy. Technol. Assess.* **2022**, *50*, 101808. DOI
21. Cárdenas, B.; León, N. High temperature latent heat thermal energy storage: phase change materials, design considerations and performance enhancement techniques. *Renew. Sustain. Energy. Rev.* **2013**, *27*, 724-37. DOI
22. Reddy, V. J.; Ghazali, M. F.; Kumarasamy, S. Advancements in phase change materials for energy-efficient building construction: a comprehensive review. *J. Energy. Storage.* **2024**, *81*, 110494. DOI
23. Klemenčič, E.; Slavinec, M. Liquid crystals as phase change materials for thermal stabilization. *Adv. Cond. Matter. Phys.* **2018**, *2018*, 1-8. DOI
24. Rojas, E.; Bayón, R.; Zarza, E. Liquid crystals: a different approach for storing latent energy in a DSG plant. *Energy. Procedia.* **2015**, *69*, 1014-22. DOI
25. Lagerwall, S. T. On some important chapters in the history of liquid crystals. *Liq. Cryst.* **2013**, *40*, 1698-729. DOI
26. Singh, S. Phase transitions in liquid crystals. *Phys. Rep.* **2000**, *324*, 107-269. DOI
27. Stephen, M. J.; Straley, J. P. Physics of liquid crystals. *Rev. Mod. Phys.* **1974**, *46*, 617-704. DOI
28. Huang, Y.; Gui, S. Factors affecting the structure of lyotropic liquid crystals and the correlation between structure and drug diffusion. *RSC. Adv.* **2018**, *8*, 6978-87. DOI PubMed PMC
29. P, P.; Malik, P.; Supreet; Kumar, A.; Castagna, R.; Singh, G. Recent advances and future perspectives on nanoparticles-controlled alignment of liquid crystals for displays and other photonic devices. *Crit. Rev. Solid. State. Mater. Sci.* **2023**, *48*, 57-92. DOI
30. Jung, J.; Park, H.; Jung, H. Y.; et al. Recent progress in liquid crystal devices and materials of TFT-LCDs. *J. Soc. Inf. Display.* **2024**, *25*, 121-42. DOI
31. Chen, H. W.; Lee, J. H.; Lin, B. Y.; Chen, S.; Wu, S. T. Liquid crystal display and organic light-emitting diode display: present status and future perspectives. *Light. Sci. Appl.* **2018**, *7*, 17168. DOI PubMed PMC
32. Wang, D.; Liu, C.; Lin, S.; Wang, Q. Holographic display technology based on liquid crystal device. *J. Soc. Inf. Display.* **2020**, *28*, 136-47. DOI
33. Carlton, R. J.; Hunter, J. T.; Miller, D. S.; et al. Chemical and biological sensing using liquid crystals. *Liq. Cryst. Rev.* **2013**, *1*, 29-51. DOI PubMed PMC
34. Popov, P.; Mann, E. K.; Jákli, A. Thermotropic liquid crystal films for biosensors and beyond. *J. Mater. Chem. B.* **2017**, *5*, 5061-78. DOI PubMed
35. Pani, I.; Sil, S.; Pal, S. K. Liquid crystal biosensors: a new therapeutic window to point-of-care diagnostics. *Langmuir* **2023**, *39*, 909-17. DOI PubMed
36. Bayón, R.; Coco, S.; Barcenilla, M.; et al. Feasibility of storing latent heat with liquid crystals. Proof of concept at lab scale. *Appl. Sci.* **2016**, *6*, 121. DOI
37. Lee, J. J. C.; Sugiarto, S.; Ong, P. J.; et al. Lignin-g-polycaprolactone as a form-stable phase change material for thermal energy storage application. *J. Energy. Storage.* **2022**, *56*, 106118. DOI
38. Soo, X. Y. D.; Muiruri, J. K.; Yeo, J. C. C.; et al. Polyethylene glycol/polylactic acid block co-polymers as solid-solid phase change materials. *SmartMat* **2023**, *4*, e1188. DOI
39. Ong, P. J.; Png, Z. M.; Debbie, S. X. Y.; et al. Surface modification of microencapsulated phase change materials with nanostructures for enhancement of their thermal conductivity. *Mater. Chem. Phys.* **2022**, *277*, 125438. DOI
40. Jin, O. P.; Leow, Y.; Yun Debbie Soo, X.; et al. Valorization of spent coffee grounds: a sustainable resource for bio-based phase change materials for thermal energy storage. *Waste. Manag.* **2023**, *157*, 339-47. DOI
41. Ong, P. J.; Goh, S. H. A.; Leow, Y.; et al. Valorization of coconut peat to develop a novel shape-stabilized phase change material for thermal energy storage. *J. Clean. Prod.* **2024**, *446*, 141468. DOI
42. Yu, P.; Zheng, J.; He, Z.; Wang, D.; Zhang, H. Energy saving phase change energy storage thermochromic liquid crystal display. *Opt. Mater.* **2023**, *142*, 113999. DOI
43. Zhou, L.; Liu, S.; Miao, X.; et al. Advancements and applications of liquid crystal/polymer composite films. *ACS. Mater. Lett.* **2023**, *5*, 2760-75. DOI
44. Mac, F. N.; Schrettl, S.; Tito, N. B.; et al. Reversible microscale assembly of nanoparticles driven by the phase transition of a thermotropic liquid crystal. *ACS. Nano.* **2023**, *17*, 9906-18. DOI PubMed PMC
45. Li, G.; Zhang, X.; Wang, J.; Fang, J. From anisotropic graphene aerogels to electron- and photo-driven phase change composites. *J. Mater. Chem. A.* **2016**, *4*, 17042-9. DOI
46. Zhao, Y.; Zheng, J.; Zhao, Y.; et al. Multi-field driven thermochromic films with phase change energy storage properties. *Dyes. Pigments.* **2023**, *208*, 110759. DOI

47. Sheng, M.; Li, J.; Jiang, X.; et al. Biomimetic solid-liquid transition structural dye-doped liquid crystal/phase-change-material microcapsules designed for wearable bistable electrochromic fabric. *ACS. Appl. Mater. Interfaces.* **2021**, *13*, 33282-90. DOI
48. Ye, Y.; Guo, L.; Zhong, T. A review of developments in polymer stabilized liquid crystals. *Polymers* **2023**, *15*, 2962. DOI PubMed PMC
49. Shibaev, V. P.; Bobrovsky, A. Y. Liquid crystalline polymers: development trends and photocontrollable materials. *Russ. Chem. Rev.* **2017**, *86*, 1024-72. DOI
50. Lyu, X.; Xiao, A.; Shi, D.; et al. Liquid crystalline polymers: Discovery, development, and the future. *Polymer* **2020**, *202*, 122740. DOI
51. Shen, W.; Li, G. Recent progress in liquid crystal-based smart windows: materials, structures, and design. *Laser. Photonics. Rev.* **2023**, *17*, 2200207. DOI
52. Collyer, A. A. Liquid crystal polymers: from structures to applications. London, New York: Elsevier; 1992. DOI
53. Shibaev, V. P.; Platé, N. A. Thermotropic liquid-crystalline polymers with mesogenic side groups. In: Platé, N. A.; editors, Liquid Crystal Polymers II/III. Berlin Heidelberg: Springer; 1984, pp. 173-252. DOI
54. Park, G. T.; Chang, J. H.; Lim, A. R. Thermotropic liquid crystalline polymers with various alkoxy side groups: thermal properties and molecular dynamics. *Polymers* **2019**, *11*, 992. DOI PubMed PMC
55. Zeng, L.; Li, R.; Chen, P.; Xu, J.; Liu, P. Synthesis and characterization of thermotropic liquid crystalline polyarylate with ether ether ketone segments in the main chain. *J. Appl. Polym. Sci.* **2016**, *133*, app.43800. DOI
56. Sadeghi, G. Energy storage on demand: thermal energy storage development, materials, design, and integration challenges. *Energy. Storage. Mater.* **2022**, *46*, 192-222. DOI
57. Konuklu, Y.; Ostry, M.; Paksoy, H. O.; Charvat, P. Review on using microencapsulated phase change materials (PCM) in building applications. *Energy. Build.* **2015**, *106*, 134-55. DOI
58. Pielichowska, K.; Pielichowski, K. Phase change materials for thermal energy storage. *Prog. Mater. Sci.* **2014**, *65*, 67-123. DOI
59. Sharshir, S. W.; Joseph, A.; Elsharkawy, M.; et al. Thermal energy storage using phase change materials in building applications: A review of the recent development. *Energy. Build.* **2023**, *285*, 112908. DOI
60. Jayathunga, D.; Karunathilake, H.; Narayana, M.; Witharana, S. Phase change material (PCM) candidates for latent heat thermal energy storage (LHTES) in concentrated solar power (CSP) based thermal applications - A review. *Renew. Sustain. Energy. Rev.* **2024**, *189*, 113904. DOI
61. Gu, H.; Chen, Y.; Yao, X.; Huang, L.; Zou, D. Review on heat pump (HP) coupled with phase change material (PCM) for thermal energy storage. *Chem. Eng. J.* **2023**, *455*, 140701. DOI
62. Freeman, T. B.; Foster, K. E.; Troxler, C. J.; et al. Advanced materials and additive manufacturing for phase change thermal energy storage and management: a review. *Adv. Energy. Mater.* **2023**, *13*, 2204208. DOI
63. Sheikh, Y.; Hamdan, M. O.; Sakhi, S. A review on micro-encapsulated phase change materials (EPCM) used for thermal management and energy storage systems: fundamentals, materials, synthesis and applications. *J. Energy. Storage.* **2023**, *72*, 108472. DOI
64. Liu, C.; Xiao, T.; Zhao, J.; et al. Polymer engineering in phase change thermal storage materials. *Renew. Sustain. Energy. Rev.* **2023**, *188*, 113814. DOI
65. Esteves, C.; Ramou, E.; Porteira, A. R. P.; Barbosa, A. J. M.; Roque, A. C. A. Seeing the unseen: the role of liquid crystals in gas-sensing technologies. *Adv. Opt. Mater.* **2020**, *8*, 1902117. DOI PubMed PMC
66. Nesterkina, M.; Kravchenko, I.; Hirsch, A. K. H.; Lehr, C. M. Thermotropic liquid crystals in drug delivery: a versatile carrier for controlled release. *Eur. J. Pharm. Biopharm.* **2024**, *200*, 114343. DOI PubMed
67. Zhang, Z.; Yang, X.; Zhao, Y.; Ye, F.; Shang, L. Liquid crystal materials for biomedical applications. *Adv. Mater.* **2023**, *35*, e2300220. DOI
68. Wang, Z.; Xu, T.; Noel, A.; Chen, Y. C.; Liu, T. Applications of liquid crystals in biosensing. *Soft. Matter.* **2021**, *17*, 4675-702. DOI
69. Zhang, W.; Froyen, A. A. F.; Schenning, A. P. H. J.; Zhou, G.; Debije, M. G.; de Haan, L. T. Temperature-responsive photonic devices based on cholesteric liquid crystals. *Adv. Photon. Res.* **2021**, *2*, 2100016. DOI
70. Yin, K.; Hsiang, E. L.; Zou, J.; et al. Advanced liquid crystal devices for augmented reality and virtual reality displays: principles and applications. *Light. Sci. Appl.* **2022**, *11*, 161. DOI PubMed PMC
71. Yu, C.; Konlan, J.; Li, G. Energy harvesting and electricity production through dissolved carbon dioxide by connecting two form-stable phase change materials. *J. Mater. Chem. A.* **2024**, *12*, 7943-55. DOI
72. Rea, J. E.; Oshman, C. J.; Olsen, M. L.; et al. Performance modeling and techno-economic analysis of a modular concentrated solar power tower with latent heat storage. *Appl. Energy.* **2018**, *217*, 143-52. DOI
73. Cao, J.; Sim, Y.; Tan, X. Y.; et al. Upcycling silicon photovoltaic waste into thermoelectrics. *Adv. Mater.* **2022**, *34*, e2110518. DOI
74. Zheng, J.; Solco, S. F. D.; Wong, C. J. E.; et al. Integrating recyclable polymers into thermoelectric devices for green electronics. *J. Mater. Chem. A.* **2022**, *10*, 19787-96. DOI
75. Zhu, Q.; Yildirim, E.; Wang, X.; et al. Effect of substituents in sulfoxides on the enhancement of thermoelectric properties of PEDOT:PSS: experimental and modelling evidence. *Mol. Syst. Des. Eng.* **2020**, *5*, 976-84. DOI
76. Tang, T.; Kyaw, A. K. K.; Zhu, Q.; Xu, J. Water-dispersible conducting polyazulene and its application in thermoelectrics. *Chem. Commun.* **2020**, *56*, 9388-91. DOI PubMed
77. Yemata, T. A.; Kyaw, A. K. K.; Zheng, Y.; et al. Enhanced thermoelectric performance of poly(3,4-ethylenedioxythiophene):poly(4-

styrenesulfonate) (PEDOT:PSS) with long-term humidity stability via sequential treatment with trifluoroacetic acid. *Polym. Int.* **2020**, *69*, 84-92. DOI

78. Cao, J.; Zheng, J.; Liu, H.; et al. Flexible elemental thermoelectrics with ultra-high power density. *Mater. Today. Energy.* **2022**, *25*, 100964. DOI
79. Dong, J.; Suwardi, A.; Tan, X. Y.; et al. Challenges and opportunities in low-dimensional thermoelectric nanomaterials. *Mater. Today.* **2023**, *66*, 137-57. DOI
80. Glatzmaier, G. C.; Rea, J.; Olsen, M. L.; et al. Solar thermoelectricity via advanced latent heat storage: a cost-effective small-scale CSP application. *AIP Conf Proc* 2017;1850:030019. DOI
81. de Gennes, P. G.; Prost, J. The physics of liquid crystals. Oxford, UK: Clarendon Press; 1995. DOI
82. Labeeb, A. M.; Ibrahim, S. A.; Ward, A. A.; Abd-el-messieh, S. L. Polymer/liquid crystal nanocomposites for energy storage applications. *Polym. Eng. Sci.* **2020**, *60*, 2529-40. DOI
83. Bayón, R.; Rojas, E. Liquid crystals: a new approach for latent heat storage: 'Always liquid' phase change materials for energy storage in DSG. *Int. J. Energy. Res.* **2013**, *37*, 1737-42. DOI
84. Dominguez-Candela, I.; Zulkhairi, I.; Pintre, I.; et al. Light-responsive bent-core liquid crystals as candidates for energy conversion and storage. *J. Mater. Chem. C.* **2022**, *10*, 18200-12. DOI
85. Gupta, M.; Ashy; Abhinand Krishna, K. M. Sunlight driven *E* - *Z* isomerization of liquid crystals based on hexahydroxytriphenylene nano-templates for enhanced solid-state solar thermal energy storage. *J. Mater. Chem. A.* **2024**, *12*, 27373-80. DOI
86. Kinyanjui, M. J.; Chee, C. Y. J.; Yun, D. S. X.; et al. Recent advances of sustainable Short-chain length polyhydroxyalkanoates (Scl-PHAs) - Plant biomass composites. *Eur. Polym. J.* **2023**, *187*, 111882. DOI
87. Soo, X. Y. D.; Jia, L.; Lim, Q. F.; et al. Hydrolytic degradation and biodegradation of polylactic acid electrospun fibers. *Chemosphere* **2024**, *350*, 141186. DOI
88. Muiruri, J. K.; Chuan, Y. J. C.; Zhu, Q.; Ye, E.; Loh, X. J.; Li, Z. Sustainable mycelium-bound biocomposites: design strategies, materials properties, and emerging applications. *ACS. Sustain. Chem. Eng.* **2023**, *11*, 6801-21. DOI
89. Chua, M. H.; Toh, S. H. G.; Ong, P. J.; et al. Towards modulating the colour hues of isoindigo-based electrochromic polymers through variation of thiophene-based donor groups. *Polym. Chem.* **2022**, *13*, 967-81. DOI
90. Noël, C.; Navard, P. Liquid crystal polymers. *Prog. Polym. Sci.* **1991**, *16*, 55-110. DOI
91. Liu, Y.; Chen, J.; Qi, Y.; et al. Cross-linked liquid crystalline polybenzoxazines bearing cholesterol-based mesogen side groups. *Polymer* **2018**, *145*, 252-60. DOI
92. Cai, F.; Song, T.; Yang, B.; Lv, X.; Zhang, L.; Yu, H. Enhancement of solar thermal fuel by microphase separation and nanoconfinement of a block copolymer. *Chem. Mater.* **2021**, *33*, 9750-9. DOI
93. Yu, Z.; Feng, D.; Feng, Y.; Zhang, X. Thermal conductivity and energy storage capacity enhancement and bottleneck of shape-stabilized phase change composites with graphene foam and carbon nanotubes. *Compos. Part. A. Appl. Sci. Manuf.* **2022**, *152*, 106703. DOI
94. Belinson, M.; Groulx, D. Numerical study of a latent heat storage system's performance as a function of the phase change material's thermal conductivity. *Appl. Sci.* **2024**, *14*, 3318. DOI
95. Ye, W.; Jamshideasli, D.; Khodadadi, J. M. Improved performance of latent heat energy storage systems in response to utilization of high thermal conductivity fins. *Energies* **2023**, *16*, 1277. DOI
96. Dhaidan, N. S.; Khodadadi, J. M. Improved performance of latent heat energy storage systems utilizing high thermal conductivity fins: a review. *J. Renew. Sustain. Energy.* **2017**, *9*, 034103. DOI
97. Agarwal, A.; Sarviya, R. Characterization of commercial grade paraffin wax as latent heat storage material for solar dryers. *Mater. Today. Proc.* **2017**, *4*, 779-89. DOI
98. Zalba, B.; Marín, J. M.; Cabeza, L. F.; Mehling, H. Review on thermal energy storage with phase change: materials, heat transfer analysis and applications. *Appl. Therm. Eng.* **2003**, *23*, 251-83. DOI
99. Bharathiraja, R.; Ramkumar, T.; Selvakumar, M. Studies on the thermal characteristics of nano-enhanced paraffin wax phase change material (PCM) for thermal storage applications. *J. Energy. Storage.* **2023**, *73*, 109216. DOI
100. Konuklu, Y.; Unal, M.; Paksoy, H. O. Microencapsulation of caprylic acid with different wall materials as phase change material for thermal energy storage. *Solar. Energy. Mater. Solar. Cells.* **2014**, *120*, 536-42. DOI
101. Sivasamy, P.; Harikrishnan, S.; Jayavel, R.; Hussain, S. I.; Kalaiselvam, S.; Lu, L. Preparation and thermal characteristics of caprylic acid based composite as phase change material for thermal energy storage. *Mater. Res. Express.* **2019**, *6*, 105051. DOI
102. Xiong, T.; Ok, Y. S.; Dissanayake, P. D.; et al. Preparation and thermal conductivity enhancement of a paraffin wax-based composite phase change material doped with garlic stem biochar microparticles. *Sci. Total. Environ.* **2022**, *827*, 154341. DOI
103. Liu, P.; Gu, X.; Bian, L.; Cheng, X.; Peng, L.; He, H. Thermal properties and enhanced thermal conductivity of capric acid/diatomite/carbon nanotube composites as form-stable phase change materials for thermal energy storage. *ACS. Omega.* **2019**, *4*, 2964-72. DOI
104. Sari, A.; Kaygusuz, K. Thermal performance of palmitic acid as a phase change energy storage material. *Energy. Convers. Manag.* **2002**, *43*, 863-76. DOI
105. Wang, J.; Xie, H.; Xin, Z.; Li, Y. Increasing the thermal conductivity of palmitic acid by the addition of carbon nanotubes. *Carbon* **2010**, *48*, 3979-86. DOI
106. Faden, M.; Höhlein, S.; Wanner, J.; König-Haagen, A.; Brüggemann, D. Review of thermophysical property data of octadecane for phase-change studies. *Materials* **2019**, *12*, 2974. DOI PubMed PMC

107. Nguyen, G. T.; Hwang, H. S.; Lee, J.; Cha, D. A.; Park, I. n-octadecane/fumed silica phase change composite as building envelope for high energy efficiency. *Nanomaterials* **2021**, *11*, 566. DOI PubMed PMC
108. Tyagi, V. V.; Buddhi, D. PCM thermal storage in buildings: a state of art. *Renew. Sustain. Energy. Rev.* **2007**, *11*, 1146-66. DOI
109. Sathyamurthy, R. Silver (Ag) based nanoparticles in paraffin wax as thermal energy storage for stepped solar still - An experimental approach. *Solar. Energy.* **2023**, *262*, 111808. DOI
110. Mehling, H.; Cabeza, L. F. Heat transfer basics. In: Heat and cold storage with PCM. Berlin, Heidelberg: Springer; 2008. DOI
111. Prabhu, B.; Valan, A. V. Stability analysis of TiO_2-Ag nanocomposite particles dispersed paraffin wax as energy storage material for solar thermal systems. *Renew. Energy.* **2020**, *152*, 358-67. DOI
112. Dixit, P.; Vennapusa, J. R.; Parvate, S.; Singh, J.; Dasari, A.; Chattopadhyay, S. Thermal buffering performance of a propyl palmitate/expanded perlite-based form-stable composite: experiment and numerical modeling in a building model. *Energy. Fuels.* **2021**, *35*, 2704-16. DOI
113. Shi, J.; Ger, M.; Liu, Y.; et al. Improving the thermal conductivity and shape-stabilization of phase change materials using nanographite additives. *Carbon* **2013**, *51*, 365-72. DOI
114. Hirano, S.; Saitoh, T. S.; Oya, M.; Yamazaki, M. Temperature dependence of thermophysical properties of disodium hydrogenphosphate dodecahydrate. *J. Thermophys. Heat. Transfer.* **2001**, *15*, 340-6. DOI
115. Xiao, X.; Zhang, P.; Li, M. Effective thermal conductivity of open-cell metal foams impregnated with pure paraffin for latent heat storage. *Int. J. Therm. Sci.* **2014**, *81*, 94-105. DOI
116. Ndukwu, M. C.; Bennamoun, L. Potential of integrating $Na_2SO_4 \cdot 10H_2O$ pellets in solar drying system. *Dry. Technol.* **2018**, *36*, 1017-30. DOI
117. Tao, W.; Kong, X.; Bao, A.; Fan, C.; Zhang, Y. Preparation and phase change performance of graphene oxide and silica composite $Na_2SO_4 \cdot 10H_2O$ phase change materials (PCMs) as thermal energy storage materials. *Materials* **2020**, *13*, 5186. DOI PubMed PMC
118. Hasnain, S. Review on sustainable thermal energy storage technologies, Part I: heat storage materials and techniques. *Energy. Convers. Manag.* **1998**, *39*, 1127-38. DOI
119. Zhang, L.; Zhou, K.; Wei, Q.; et al. Thermal conductivity enhancement of phase change materials with 3D porous diamond foam for thermal energy storage. *Appl. Energy.* **2019**, *233-4*, 208-19. DOI
120. Farid, M. M.; Khudhair, A. M.; Razack, S. A. K.; Al-Hallaj, S. A review on phase change energy storage: materials and applications. *Energy. Convers. Manag.* **2004**, *45*, 1597-615. DOI
121. Dong, K.; Sheng, N.; Zou, D.; Wang, C.; Yi, X.; Nomura, T. High anisotropic thermal conductivity, long durability form-stable phase change composite enhanced by a carbon fiber network structure. *Crystals* **2021**, *11*, 230. DOI
122. Ling, Z.; Liu, J.; Wang, Q.; Lin, W.; Fang, X.; Zhang, Z. $MgCl_2 \cdot 6H_2O$-$Mg(NO_3)_2 \cdot 6H_2O$ eutectic/SiO_2 composite phase change material with improved thermal reliability and enhanced thermal conductivity. *Solar. Energy. Mater. Solar. Cells.* **2017**, *172*, 195-201. DOI
123. Mao, J.; Hou, P.; Liu, R.; Chen, F.; Dong, X. Preparation and thermal properties of SAT-CMC-DSP/EG composite as phase change material. *Appl. Therm. Eng.* **2017**, *119*, 585-92. DOI
124. Williams, J. D.; Peterson, G. P. A review of thermal property enhancements of low-temperature nano-enhanced phase change materials. *Nanomaterials* **2021**, *11*, 2578. DOI PubMed PMC
125. Li, M. A nano-graphite/paraffin phase change material with high thermal conductivity. *Appl. Energy.* **2013**, *106*, 25-30. DOI
126. Jebasingh B, Valan Arasu A. A comprehensive review on latent heat and thermal conductivity of nanoparticle dispersed phase change material for low-temperature applications. *Energy. Storage. Mater.* **2020**, *24*, 52-74. DOI
127. Shahid, U. B.; Abdala, A. A critical review of phase change material composite performance through Figure-of-Merit analysis: graphene vs boron nitride. *Energy. Storage. Mater.* **2021**, *34*, 365-87. DOI
128. Shao, L.; Raghavan, A.; Kim, G.; et al. Figure-of-merit for phase-change materials used in thermal management. *Int. J. Heat. Mass. Transfer.* **2016**, *101*, 764-71. DOI
129. Tripathi, P. M.; Marconnet, A. M. A new thermal management figure of merit for design of thermal energy storage with phase change materials. *Int. J. Heat. Mass. Transfer.* **2024**, *220*, 124952. DOI
130. Ahlers, G.; Cannell, D. S.; Berge, L. I.; Sakurai, S. Thermal conductivity of the nematic liquid crystal 4-n-pentyl-4'-cyanobiphenyl. *Phys. Rev. E. Stat. Phys. Plasmas. Fluids. Relat. Interdiscip. Top.* **1994**, *49*, 545-53. DOI
131. Mercuri, F.; Zammit, U.; Marinelli, M. Effect of the nematic range on the critical behavior and anisotropy of the heat transport parameters at the smectic- A - nematic phase transition. *Phys. Rev. E.* **1998**, *57*, 596-602. DOI
132. Abdulkarim-talaq, M.; Hassan, K. T.; Hameed, D. A. Improvement of thermal conductivity of novel asymmetric dimeric coumarin liquid crystal by doping with boron nitride and aluminium oxide nanoparticles. *Mater. Chem. Phys.* **2023**, *297*, 127367. DOI
133. Collings, P. J.; Goodby, J. W. Introduction to liquid crystals: chemistry and physics. Boca Raton, FL: CRC Press; 2020. DOI
134. Brouckaert, N.; Podoliak, N.; Orlova, T.; et al. Nanoparticle-induced property changes in nematic liquid crystals. *Nanomaterials* **2022**, *12*, 341. DOI PubMed PMC
135. Kashyap, B.; Saini, A.; Rastogi, A. Enhancing liquid crystal properties through nanoparticle doping: a mini review. *Asian. J. Chem.* **2024**, *36*, 543-8. DOI
136. Orlandi, S.; Benini, E.; Miglioli, I.; Evans, D. R.; Reshetnyak, V.; Zannoni, C. Doping liquid crystals with nanoparticles. A computer simulation of the effects of nanoparticle shape. *Phys. Chem. Chem. Phys.* **2016**, *18*, 2428-41. DOI PubMed
137. Lee, H. L.; Mohammed, I. A.; Belmahi, M.; Assouar, M. B.; Rinnert, H.; Alnot, M. Thermal and optical properties of CdS

Nanoparticles in thermotropic liquid crystal monomers. *Materials* **2010**, *3*, 2069-86. DOI PMC

138. Montazami, R.; Spillmann, C. M.; Naciri, J.; Ratna, B. R. Enhanced thermomechanical properties of a nematic liquid crystal elastomer doped with gold nanoparticles. *Sensor. Actuat. A. Phys.* **2012**, *178*, 175-8. DOI
139. Özgan, Ş.; Eskalen, H.; Tapkıranlı, Y. Thermal and electro-optic properties of graphene oxide-doped hexylcyanobiphenyl liquid crystal. *J. Theor. Appl. Phys.* **2018**, *12*, 169-76. DOI
140. Mohammad, A.; Hassan, K. T.; Hameed, D. A. Liquid crystalline behaviour of new dimers containing coumarin and biphenyl moieties and enhancement of their thermal conductivity: liquid crystal-nanoparticles. *Liq. Cryst.* **2023**, *50*, 881-90. DOI
141. Singh, S. Impact of dispersion of nanoscale particles on the properties of nematic liquid crystals. *Crystals* **2019**, *9*, 475. DOI
142. Yeo, R. J.; Yeo, J. C. C.; Yu, T. S.; et al. Core-shell micro- and nano-structures for the modification of light-surface interactions. *Adv. Opt. Mater.* **2024**, *12*, 2301955. DOI
143. Yeo, R.; Wu, W.; Tomczak, N.; et al. Tailoring surface reflectance through nanostructured materials design for energy-efficient applications. *Mater. Today. Chem.* **2023**, *30*, 101593. DOI
144. Zhang, T.; Luo, T. Role of chain morphology and stiffness in thermal conductivity of amorphous polymers. *J. Phys. Chem. B.* **2016**, *120*, 803-12. DOI PubMed
145. Soo, X. Y. D.; Muiruri, J. K.; Wu, W. Y.; et al. Bio-polyethylene and polyethylene biocomposites: an alternative toward a sustainable future. *Macromol. Rapid. Commun.* **2024**, *45*, e2400064. DOI
146. Wang, S.; Muiruri, J. K.; Soo, X. Y. D.; et al. Bio-polypropylene and polypropylene-based biocomposites: solutions for a sustainable future. *Chem. Asian. J.* **2023**, *18*, e202200972. DOI
147. Png, Z. M.; Wang, C.; Yeo, J. C. C.; et al. Stimuli-responsive structure-property switchable polymer materials. *Mol. Syst. Des. Eng.* **2023**, *8*, 1097-129. DOI
148. Lv, G.; Shen, C.; Shan, N.; et al. Odd-even effect on the thermal conductivity of liquid crystalline epoxy resins. *Proc. Natl. Acad. Sci. USA.* **2022**, *119*, e2211151119. DOI PubMed PMC
149. Li, Y.; Gong, C.; Li, C.; et al. Liquid crystalline texture and hydrogen bond on the thermal conductivities of intrinsic thermal conductive polymer films. *J. Mater. Sci. Technol.* **2021**, *82*, 250-6. DOI
150. Koda, T.; Toyoshima, T.; Komatsu, T.; Takezawa, Y.; Nishioka, A.; Miyata, K. Ordering simulation of high thermal conductivity epoxy resins. *Polym. J.* **2013**, *45*, 444-8. DOI
151. Zhang, Q.; Chen, G.; Wu, K.; Shi, J.; Liang, L.; Lu, M. Biphenyl liquid crystal epoxy containing flexible chain: synthesis and thermal properties. *J. Appl. Polym. Sci.* **2020**, *137*, 49143. DOI
152. Rashidi, V.; Coyle, E. J.; Sebeck, K.; Kieffer, J.; Pipe, K. P. Thermal conductance in cross-linked polymers: effects of non-bonding interactions. *J. Phys. Chem. B.* **2017**, *121*, 4600-9. DOI PubMed
153. Kim, G. H.; Lee, D.; Shanker, A.; et al. High thermal conductivity in amorphous polymer blends by engineered interchain interactions. *Nat. Mater.* **2015**, *14*, 295-300. DOI
154. Zhang, L.; Ruesch, M.; Zhang, X.; Bai, Z.; Liu, L. Tuning thermal conductivity of crystalline polymer nanofibers by interchain hydrogen bonding. *RSC. Adv.* **2015**, *5*, 87981-6. DOI
155. Yuan, S. J.; Peng, Z. Q.; Rong, M. Z.; Zhang, M. Q. Enhancement of intrinsic thermal conductivity of liquid crystalline epoxy through the strategy of interlocked polymer networks. *Mater. Chem. Front.* **2022**, *6*, 1137-49. DOI
156. Singh, V.; Bougher, T. L.; Weathers, A.; et al. High thermal conductivity of chain-oriented amorphous polythiophene. *Nat. Nanotechnol.* **2014**, *9*, 384-90. DOI
157. Leung, S. N.; Khan, M. O.; Naguib, H.; Dawson, F. Multifunctional polymer nanocomposites with uniaxially aligned liquid crystal polymer fibrils and graphene nanoplatelets. *Appl. Phys. Lett.* **2014**, *104*, 081904. DOI
158. Liu, J.; Yang, R. Tuning the thermal conductivity of polymers with mechanical strains. *Phys. Rev. B.* **2010**, *81*, 174122. DOI
159. Bai, L.; Zhao, X.; Bao, R.; Liu, Z.; Yang, M.; Yang, W. Effect of temperature, crystallinity and molecular chain orientation on the thermal conductivity of polymers: a case study of PLLA. *J. Mater. Sci.* **2018**, *53*, 10543-53. DOI
160. Kim, D. G.; Kim, Y. H.; Shin, T. J.; et al. Highly anisotropic thermal conductivity of discotic nematic liquid crystalline films with homeotropic alignment. *Chem. Commun.* **2017**, *53*, 8227-30. DOI
161. Karyappa, R.; Hashimoto, M. Chocolate-based ink three-dimensional printing (Ci3DP). *Sci. Rep.* **2019**, *9*, 14178. DOI PubMed PMC
162. Ghodbane, S. A.; Murthy, N. S.; Dunn, M. G.; Kohn, J. Achieving molecular orientation in thermally extruded 3D printed objects. *Biofabrication* **2019**, *11*, 045004. DOI PubMed PMC
163. Loskot, J.; Jezbera, D.; Loskot, R.; et al. Influence of print speed on the microstructure, morphology, and mechanical properties of 3D-printed PETG products. *Polym. Test.* **2023**, *123*, 108055. DOI
164. Seshadri, B.; Hischier, I.; Masania, K.; Schlueter, A. 3D printed liquid crystal polymer thermosiphon for heat transfer under vacuum. *Adv. Mater. Technol.* **2023**, *8*, 2300403. DOI
165. Luo, F.; Yang, S.; Yan, P.; et al. Orientation behavior and thermal conductivity of liquid crystal polymer composites based on three-dimensional printing. *Compos. Part. A. Appl. Sci. Manuf.* **2022**, *160*, 107059. DOI
166. Houriet, C.; Damodaran, V.; Mascolo, C.; Gantenbein, S.; Peeters, D.; Masania, K. 3D printing of flow-inspired anisotropic patterns with liquid crystalline polymers. *Adv. Mater.* **2024**, *36*, e2307444. DOI PubMed
167. Johann, K. S.; Böhm, F.; Kapernaum, N.; Giesselmann, F.; Bonten, C. Orientation of liquid crystalline polymers after filament extrusion and after passing through a 3D printer nozzle. *ACS. Appl. Polym. Mater.* **2024**, *6*, 10006-18. DOI

168. Karyappa, R.; Ohno, A.; Hashimoto, M. Immersion precipitation 3D printing (ip3DP). *Mater. Horiz.* **2019**, *6*, 1834-44. DOI
169. Karyappa, R.; Liu, H.; Zhu, Q.; Hashimoto, M. Printability of poly(lactic acid) ink by embedded 3D printing via immersion precipitation. *ACS. Appl. Mater. Interfaces.* **2023**, *15*, 21575-84. DOI
170. Karyappa, R.; Hashimoto, M. Freeform polymer precipitation in microparticulate gels. *ACS. Appl. Polym. Mater.* **2021**, *3*, 908-19. DOI
171. Karyappa, R.; Zhang, D.; Zhu, Q.; Ji, R.; Suwardi, A.; Liu, H. Newtonian liquid-assisted material extrusion 3D printing: progress, challenges and future perspectives. *Addit. Manuf.* **2024**, *79*, 103903. DOI
172. Wang, S.; Ong, P. J.; Liu, S.; et al. Recent advances in host-guest supramolecular hydrogels for biomedical applications. *Chem. Asian. J.* **2022**, *17*, e202200608. DOI
173. Zhu, H.; Mah, J. Q. J.; Wang, C. G.; et al. Flexible polymeric patch based nanotherapeutics against non-cancer therapy. *Bioact. Mater.* **2022**, *18*, 471-91. DOI PubMed PMC
174. Liu, M.; Chen, Y.; Zhu, Q.; et al. Antioxidant thermogelling formulation for burn wound healing. *Chem. Asian. J.* **2022**, *17*, e202200396. DOI
175. Wei, F.; Cheng, B.; Chew, L. T.; et al. Grain distribution characteristics and effect of diverse size distribution on the Hall-Petch relationship for additively manufactured metal alloys. *J. Mater. Res. Technol.* **2022**, *20*, 4130-6. DOI
176. Wu, J.; Wu, W.; Wang, S.; et al. Polymer electrolytes for flexible zinc-air batteries: recent progress and future directions. *Nano. Res.* **2024**, *17*, 6058-79. DOI
177. Li, M.; Gong, P.; Zhang, Z.; et al. Electric-field-aligned liquid crystal polymer for doubling anisotropic thermal conductivity. *Commun. Mater.* **2024**, *5*, 455. DOI
178. Wang, M.; Wang, J.; Yang, H.; et al. Homeotropically-aligned main-chain and side-on liquid crystalline elastomer films with high anisotropic thermal conductivities. *Chem. Commun.* **2016**, *52*, 4313-6. DOI
179. Kurabayashi, K. Anisotropic thermal energy transport in polarized liquid crystalline (LC) polymers under electric fields. *Microsc. Thermophys. Eng.* **2003**, *7*, 87-99. DOI
180. Shin, J.; Kang, M.; Tsai, T.; Leal, C.; Braun, P. V.; Cahill, D. G. Thermally functional liquid crystal networks by magnetic field driven molecular orientation. *ACS. Macro. Lett.* **2016**, *5*, 955-60. DOI
181. Harada, M.; Ochi, M.; Tobita, M.; et al. Thermomechanical properties of liquid-crystalline epoxy networks arranged by a magnetic field. *J. Polym. Sci. B. Polym. Phys.* **2004**, *42*, 758-65. DOI
182. Varela-Domínguez, N.; López-Bueno, C.; López-Moreno, A.; et al. Light-induced bi-directional switching of thermal conductivity in azobenzene-doped liquid crystal mesophases. *J. Mater. Chem. C. Mater.* **2023**, *11*, 4588-94. DOI PubMed PMC
183. Shin, J.; Sung, J.; Kang, M.; et al. Light-triggered thermal conductivity switching in azobenzene polymers. *Proc. Natl. Acad. Sci. USA.* **2019**, *116*, 5973-8. DOI
184. Dai, M.; Picot, O. T.; Verjans, J. M.; et al. Humidity-responsive bilayer actuators based on a liquid-crystalline polymer network. *ACS. Appl. Mater. Interfaces.* **2013**, *5*, 4945-50. DOI
185. Lan, R.; Shen, W.; Yao, W.; Chen, J.; Chen, X.; Yang, H. Bioinspired humidity-responsive liquid crystalline materials: from adaptive soft actuators to visualized sensors and detectors. *Mater. Horiz.* **2023**, *10*, 2824-44. DOI
186. Ji, Y.; Yang, B.; Cai, F.; Yu, H. Regulating surface topography of liquid-crystalline polymers by external stimuli. *Macro. Chem. Phys.* **2022**, *223*, 2100418. DOI
187. Gupta, M.; Ashy Solar thermal energy storage systems based on discotic nematic liquid crystals that can efficiently charge and discharge below 0 °C. *Adv. Energy. Mater.* **2024**, *14*, 2303845. DOI
188. Liu, J.; Li, Z.; Lv, C.; et al. Electrocatalytic upgrading of nitrogenous wastes into value-added chemicals: a review. *Mater. Today.* **2024**, *73*, 208-59. DOI
189. Hu, E.; Jia, B. E.; Zhu, Q.; et al. Engineering high voltage aqueous aluminum-ion batteries. *Small* **2024**, e2309252. DOI
190. Jia, B.; Hu, E.; Hu, Z.; et al. Laminated tin-aluminum anodes to build practical aqueous aluminum batteries. *Energy. Storage. Mater.* **2024**, *65*, 103141. DOI
191. Yeo, R. J.; Sng, A.; Wang, C.; Tao, L.; Zhu, Q.; Bu, J. Strategies for heavy metals immobilization in municipal solid waste incineration bottom ash: a critical review. *Rev. Environ. Sci. Biotechnol.* **2024**, *23*, 503-68. DOI
192. Wu, W. Y.; Zhang, M.; Wang, C.; Tao, L.; Bu, J.; Zhu, Q. Harnessing ash for sustainable CO_2 absorption: current strategies and future prospects. *Chem. Asian. J.* **2024**, *19*, e202400180. DOI
193. Soo, X. Y. D.; Lee, J. J. C.; Wu, W.; et al. Advancements in CO_2 capture by absorption and adsorption: a comprehensive review. *J. CO2. Util.* **2024**, *81*, 102727. DOI
194. Soo, X. Y. D.; Zhang, D.; Tan, S. Y.; et al. Ultra-high performance thermochromic polymers via a solid-solid phase transition mechanism and their applications. *Adv. Mater.* **2024**, *36*, e2405430. DOI
195. Kalinin, D.; Abercrombie, J. The applications of machine learning in the study of liquid crystals: a review. *J. Stud. Res.* **2023**, *12*, 3983. DOI
196. Maeda, H.; Wu, S.; Marui, R.; et al. Discovery of liquid crystalline polymers with high thermal conductivity using machine learning. *ChemRxiv* **2024**. DOI
197. Wu, D.; Ni, B.; Liu, Y.; Chen, S.; Zhang, H. Preparation and characterization of side-chain liquid crystal polymer/paraffin composites as form-stable phase change materials. *J. Mater. Chem. A.* **2015**, *3*, 9645-57. DOI
198. Han, G. G. D.; Li, H.; Grossman, J. C. Optically-controlled long-term storage and release of thermal energy in phase-change

materials. *Nat. Commun.* **2017**, *8*, 1446. DOI PubMed PMC

199. Wu, S.; Kondo, Y.; Kakimoto, M.; et al. Machine-learning-assisted discovery of polymers with high thermal conductivity using a molecular design algorithm. *NPJ. Comput. Mater.* **2019**, *5*, 203. DOI
200. Zhu, M.; Song, H.; Yu, Q.; Chen, J.; Zhang, H. Machine-learning-driven discovery of polymers molecular structures with high thermal conductivity. *Int. J. Heat. Mass. Transfer.* **2020**, *162*, 120381. DOI
201. Inokuchi, T.; Okamoto, R.; Arai, N. Predicting molecular ordering in a binary liquid crystal using machine learning. *Liq. Cryst.* **2020**, *47*, 438-48. DOI
202. Osiecka-Drewniak, N.; Drzewicz, A.; Juszyńska-Gałązka, E. Machine learning studies for liquid crystal texture recognition. *Liq. Cryst.* **2024**, *51*, 255-64. DOI